

Note Technique LNHB/01/09/A

**ETNA (Efficiency Transfer for Nuclide
Activity measurements)**

**Software for efficiency transfer and
coincidence summing corrections
in gamma-ray spectrometry**

Marie-Christine Lépy, Marie-Martine Bé, François Piton

**April 2001
Revised February 2004**

**ETNA (Efficiency Transfer for Nuclide Activity measurements)
Software for efficiency transfer and coincidence summing
corrections in gamma-ray spectrometry**

Marie-Christine Lépy, Marie-Martine Bé, François Piton

CONTENTS

1. Introduction.....	3
2. Efficiency transfer.....	4
2.1. Change in efficiency associated with displacement of a point source	4
2.2. Extension to the volume source.....	6
2.3. Calculation procedure.....	8
2.3.1. Integration	8
2.3.2. Distances travelled in different materials.....	9
3. Correction for coincidences.....	12
3.1. Effect of coincidences on a photon spectrum.....	13
3.2. Examples for a decay scheme with two excited levels.....	14
3.3. General case of a decay scheme with a several excited levels	16
3.3.1. Correction for a γ_{ij} line	16
3.3.2. Correction for XK lines.....	18
3.4. Special cases.....	20
3.4.1. Beta+ emission	20
3.4.2. Decay scheme with two branches	20
3.4.3. Decay scheme with one metastable level.....	20
3.5. Case of non-point samples	20
4. Description of the program.....	22
4.1. General.....	22
4.2. Calculation of efficiency transfer.....	26
4.3. Calculation of coincidence-summing corrections.....	26
5. Conclusion.....	26
6. Bibliography.....	28
APPENDIX 1 – User manual.....	30

A1_1 General	30
A1_2 Efficiency transfer	31
A1_2.1 Description of the source.....	32
A1_2.2 Description of the absorber	34
A1_2.3 Description of the detector	34
A1_2.4 Efficiency	36
A1_2.5 Processing.....	38
A1_3 Corrections for coincidence summing	40
A1_3.1 Radionuclide.....	40
A1_3.2 Geometry	40
A1_3.3 Processing.....	41
A1_4 Miscellaneous	43
A1_4.1 Updating of decay data.....	43
A1_4.2 Materials management	44
A1_4.3 Setting the threshold for calculation of coincidence corrections	45
<i>APPENDIX 2 – Definitions</i>	<i>46</i>
A2_1 Data characterising the decay scheme.....	46
A2_1.1 Gamma transition	46
A2_1.2 Gamma emission	46
A2_1.3 Internal conversion.....	46
A2_1.4 X-Ray emission following internal conversion.....	47
A2_1.5 Electron capture.....	48
A2_2 Parameters characterising the detector	48
A2_2.1 Full-energy peak efficiency.....	48
A2_2.2 Total efficiency.....	48

ETNA (Efficiency Transfer for Nuclide Activity measurements) Software for efficiency transfer and coincidence summing corrections in gamma-ray spectrometry

Marie-Christine Lépy, Marie-Martine Bé, François Piton

1. Introduction

The quality of gamma spectrometry measurement generally depends directly on the knowledge of detection efficiency with the geometrical conditions of the source-detector arrangement. As the samples commonly measured can vary greatly, calibration is not available for all the materials and packaging systems encountered. Users are therefore obliged to develop experimental methods for specific standards. These techniques are of variable reliability and require set-up times that can be incompatible with the requirements of routine measurements. In addition, in the case of short-range measurement, which is, in particular, necessary for measuring environmental samples, coincidence summing phenomena disturb the spectrum and distort the areas of the peaks, thus giving erroneous quantitative results.

ETNA (an acronym standing for Efficiency Transfer for Nuclide Activity measurements) is a program designed to overcome these two difficulties. It is a calculation facility that offers a practical and convenient solution to the problems encountered in the measurement laboratories. It can be used to calculate the efficiency of the detector under measurement conditions different from those of calibration, and to correct for coincidence summing effects. It makes it possible to greatly increase the accuracy of the results of quantitative analysis by gamma spectrometry, and avoid time-consuming measurement sequences.

The system is based on two programs previously written in FORTRAN [1-2] that have been adapted and improved, then integrated in the Windows® environment for ease of use. Databases have also been included, making it possible to record characteristics of different geometries and update data on materials and decay schemes.

2. Efficiency transfer

Change in efficiency under conditions of measurement different from those of calibration can be determined on the basis of variation of the geometrical parameters of the source-detector arrangement. By calculation, it is possible to determine the efficiency corresponding to non-point samples and/or different distances and thus establish the coincidence summing corrections.

2.1. Change in efficiency associated with displacement of a point source

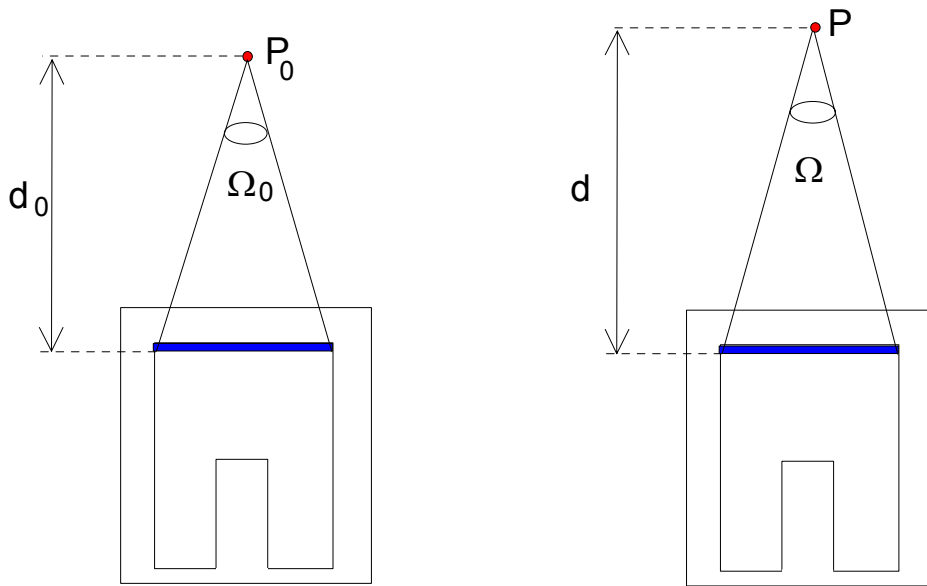


Figure 1 – Displacement of a point source along the axis of the detector

The basic case corresponds to calibration with known efficiency for a point source located at position P_0 ; at energy E , the efficiency can be expressed as the product of two terms:

$$R(E, P_0) = RI(E) \cdot \Omega(P_0),$$

where $RI(E)$ represents the intrinsic efficiency of the detector for energy E and $\Omega(P_0)$ the solid angle subtended by point P_0 and the active surface of the detector [3].

For a point located at a different distance P , the efficiency can be written, in a similar manner, as:

$$R(E, P) = RI(E) \cdot \Omega(P),$$

which makes it possible to establish the basic relationship:

$$R(E, P) = R(E, P_0) \cdot \frac{\Omega(P)}{\Omega(P_0)}$$

and to deduce the transfer coefficient as the ratio of the solid angles corresponding to the positions of measurement and calibration, P and P₀ respectively.

In polar coordinates, the solid angle, Ω(P), subtended by point P (r, φ, z_S) is written as:

$$\Omega(P) = 2 \cdot z_S \int_0^\pi \int_0^{R_D} \frac{R \cdot dR}{\left[R^2 - 2 \cdot R \cdot r \cdot \cos \varphi + r^2 + z_S^2 \right]^{3/2}}$$

where R_D is the radius of the active detection zone.

As a general rule, the calculation is made for a given coaxial cylindrical source-detector geometry and considers a detector containing a void. The solid angle is therefore calculated for two distinct parts: a solid cylinder representing the upper part of the detector and a hollow cylinder, with a height corresponding to that of the void, representing the lower part.

This purely geometrical factor needs to be supplemented both with attenuation of the incident radiation in the different materials acting as absorbers between the point of emission and the detector, F_{att}, as well as the probability of interaction in the detector, F_{abs}, as follows:

$$F_{att} = \exp\left(-\sum_{i=1}^m \mu_i \cdot \delta_i\right)$$

where μ_i is the coefficient of total attenuation per unit length, without coherent scattering, of the absorber i, and δ_i is the distance travelled in the material.

$$F_{abs} = f_1 + f_2 \cdot f'$$

where:

$$f_1 = 1 - \exp(-\mu_D \cdot \delta_{1D}) \quad f_2 = 1 - \exp(-\mu_D \cdot \delta_{2D}) \quad \text{and} \quad f' = \exp(-\mu_D \cdot (\Delta + \delta_{1D}))$$

μ_D is the total linear attenuation coefficient, without coherent scattering, of the detector material, δ_{1D} and δ_{2D} the length travelled in the active part of it before and after the central void and Δ the distance travelled in the central void.

The detector is considered here to be coaxial and the attenuation factors allowed for are due to:

- the surrounding air or other medium,
- an absorber placed between the source and the detector,
- the detector window,
- the “dead” zones of the detector (internal and external).

2.2. Extension to the volume source case

For a volume source, with cylindrical symmetry (radius R_s and thickness H_s , located at level Z_s), the solid angle expression is as follows:

$$\Omega = \frac{4}{R_s^2 \cdot H_s} \int_{Z_s}^{Z_s+H_s} h \cdot dh \int_0^{R_s} r \cdot dr \int_0^\pi d\varphi \int_0^{R_D} \frac{R \cdot dR}{[R^2 - 2 \cdot R \cdot r \cdot \cos \varphi + r^2 + h^2]^{3/2}}$$

Calculation of the effective solid angle (combination of the geometrical solid angle and the attenuation and absorption factors) is extended to sources with diameters greater than that of the detector, including Marinelli geometries, assuming that the photons enter through the side of the detector. This is obtained by dividing the source volume into domains and considering all the possible paths of interaction with the detector (top, side or bottom of detector) [4]. Thus, for a cylindrical source with a diameter greater than that of the detector, calculation of the “effective” solid angle is twofold:

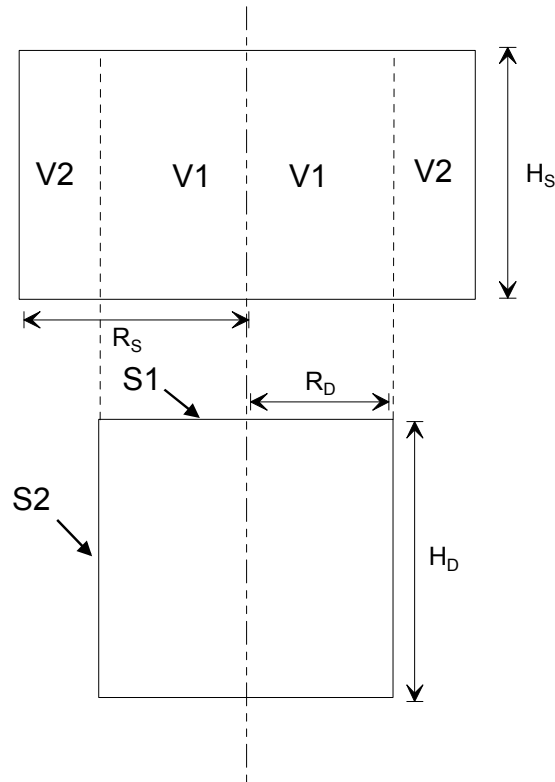


Figure 2 – Volumes and areas considered in the case of a cylindrical source

$$\bar{\Omega} = \int_{(V1+V2)S1} d\bar{\Omega} + \int_{(V2)S2} d\bar{\Omega} = \bar{\Omega}_1 + \bar{\Omega}_2$$

Where $V1$ represents the volume of the source corresponding to the detector radius, $V2$ the additional volume, $S1$ the area of the top of the detector and $S2$ the side of the detector, hence:

$$\bar{\Omega}_1 = \frac{4}{R_S^2 \cdot H_S} \int_{Z_S}^{Z_S+H_S} h \cdot dh \int_0^{R_S} r \cdot dr \int_0^\pi d\phi \int_0^{R_D} \frac{F_{att} \cdot F_{abs} \cdot R \cdot dR}{[R^2 - 2 \cdot R \cdot r \cdot \cos \phi + r^2 + h^2]^{3/2}}$$

and

$$\bar{\Omega}_2 = \frac{4 \cdot R_D}{(R_S^2 - R_D^2) \cdot H_S} \int_{Z_S}^{Z_S+H_S} dh \int_0^{R_S} r \cdot dr \int_0^{\phi_0} d\phi \int_{Z_D}^0 \frac{F_{att} \cdot F_{abs} \cdot (r \cdot \cos \phi - R_D) \cdot dz}{[R^2 - 2 \cdot R \cdot r \cdot \cos \phi + r^2 + h^2]^{3/2}}$$

where ϕ_0 is the maximum angle scanned by a point on the source on the side of the detector:

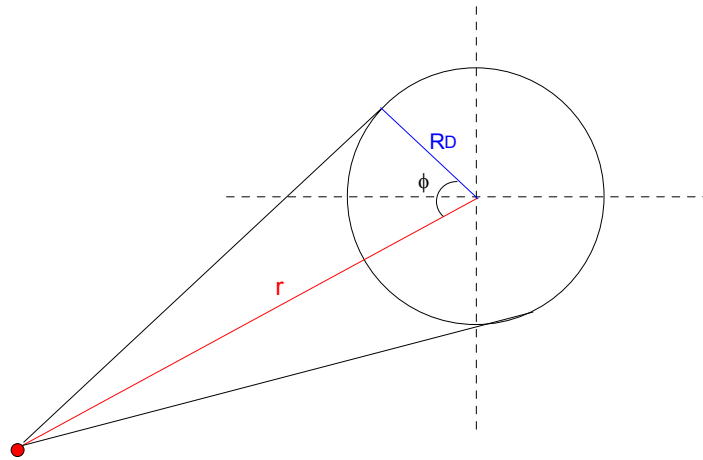


Figure 3 – Scan angle $\phi = \text{Arccos}(R_D / r)$

In the case of Marinelli geometry, the source volume is divided into five parts:

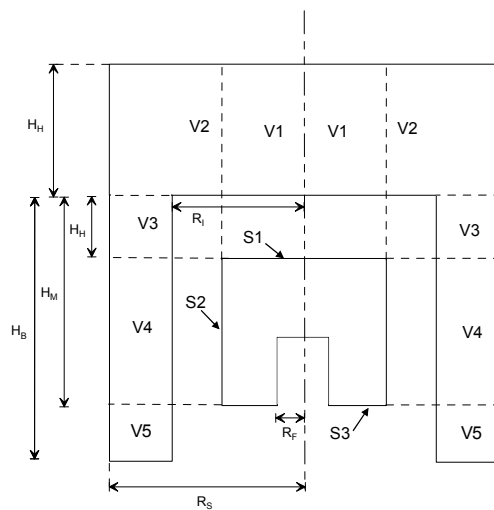


Figure 4 – Volumes and areas considered in the case of a source of the Marinelli type

$$\bar{\Omega} = \int_{(V1+V2)S1} d\bar{\Omega} + \int_{(V2)S2} d\bar{\Omega} + \int_{(V3)S1} d\bar{\Omega} + \int_{(V3+V4+V5)S2} d\bar{\Omega} + \int_{(V5)S3} d\bar{\Omega} = \bar{\Omega}_1 + \bar{\Omega}_2 + \bar{\Omega}_3 + \bar{\Omega}_4 + \bar{\Omega}_5^1$$

where

$$\bar{\Omega}_1 = \frac{4}{R_S^2 \cdot H_S} \int_{Z_S}^{Z_S+H_S} h \cdot dh \int_0^{R_S} r \cdot dr \int_0^\pi d\varphi \int_0^{R_D} \frac{F_{att} \cdot F_{abs} \cdot R \cdot dR}{[R^2 - 2 \cdot R \cdot r \cdot \cos \varphi + r^2 + h^2]^{3/2}}$$

$$\bar{\Omega}_2 = \frac{4 \cdot R_D}{(R_S^2 - R_D^2) \cdot H_S} \int_{Z_S}^{Z_S+H_S} dh \int_{R_D}^{R_S} r \cdot dr \int_0^{\phi_0} d\varphi \int_{Z_D}^0 \frac{F_{att} \cdot F_{abs} \cdot (r \cdot \cos \varphi - R_D) \cdot dz}{[R^2 - 2 \cdot R \cdot r \cdot \cos \varphi + r^2 + h^2]^{3/2}}$$

$$\bar{\Omega}_3 = \frac{4}{(R_S^2 - R_I^2) \cdot HH} \int_{Z_S+HH}^{Z_S+H_S} h \cdot dh \int_{R_I}^{R_S} r \cdot dr \int_0^\pi d\varphi \int_0^{R_D} \frac{F_{att} \cdot F_{abs} \cdot R \cdot dR}{[R^2 - 2 \cdot R \cdot r \cdot \cos \varphi + r^2 + h^2]^{3/2}}$$

$$\bar{\Omega}_4 = \frac{4 \cdot R_D}{(R_S^2 - R_I^2) \cdot (HM - HH)} \int_{Z_S+HM}^{Z_S+HH} dh \int_{R_I}^{R_S} r \cdot dr \int_0^{\phi_0} d\varphi \int_{Z_D}^0 \frac{F_{att} \cdot F_{abs} \cdot (r \cdot \cos \varphi - R_D) \cdot dz}{[R^2 - 2 \cdot R \cdot r \cdot \cos \varphi + r^2 + h^2]^{3/2}}$$

$$\bar{\Omega}_5 = \frac{4}{(R_S^2 - R_I^2) \cdot (HB - HH)} \int_{Z_S+HB}^{Z_S+HM} h \cdot dh \int_{R_I}^{R_S} r \cdot dr \int_0^\pi d\varphi \int_{R_F}^{R_D} \frac{F_{att} \cdot F_{abs} \cdot R \cdot dR}{[R^2 - 2 \cdot R \cdot r \cdot \cos \varphi + r^2 + h^2]^{3/2}}$$

In both the volume source cases, it is necessary to allow for attenuation factors corresponding to the environment of the source and its container.

2.3. Calculation procedure

2.3.1. Integration

As the effective solid angle expression cannot be solved numerically, Gauss-Legendre integration is used. For an integral with variable x, calculation corresponds to summing:

$$\int_a^b f(x) dx = \frac{(b-a)}{2} \sum_{i=1}^n w_i f(x_i)$$

where :

$$f(x_i) = \frac{(b-a)}{2} x_i + \frac{(b+a)}{2}$$

¹ This breakdown therefore makes no allowance for any photons entering from the bottom of the detector void.

x_i and w_i are respectively the roots of the Legendre polynomials and the weighting, depending on the increment of integration n whose values are tabulated [5]; in the general case, summing is made with 32 iterations. The procedure is extended to integration for a number of variables with summing in nested loops.

2.3.2. Distances travelled in different materials

All the distances necessary for the calculation are determined by the “INTERSEC” sub-program supplied by Octavian Sima (Bucarest University) [6]. This module tests whether a trajectory defined by its point of origin and its direction cosines intersects a cylinder, and calculates the corresponding path from the point of departure to the point of intersection. 12 paths are thus calculated for the disk or point source case, 14 for the cylindrical case and 19 for the Marinelli geometry case, making it possible to calculate the distances travelled in the different materials, there being 5 for the first two cases (air, window, dead zone, absorber and active zone) and 7 (source and container in addition) for the last two.

The calculation allows for the coaxial detector, with its central void, the dead zones at the front side and centre of the detection crystal, the inlet window, the detector cover, the ambient medium (air or other) and possibly the presence of a horizontal absorber between the source and the detector, the container of the source and its matrix. Figure 5 shows the various useful geometrical parameters (dimensions relative to upper plane of active zone of detector and radii) as referenced in the software, with a germanium detector. If a screen is present, it is also necessary to add dimensions Z_{12} and Z_{13} corresponding to the top and bottom of the absorber respectively.

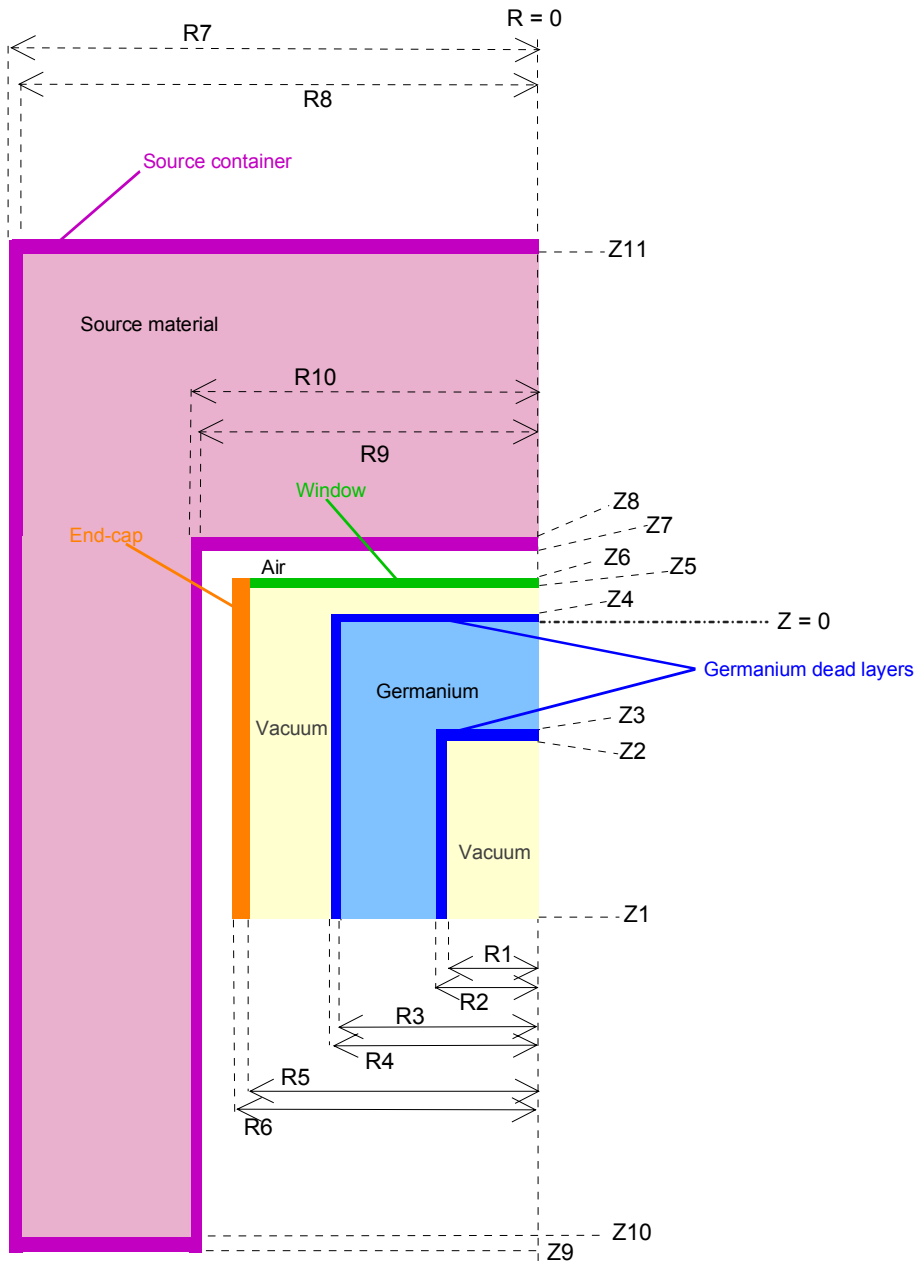
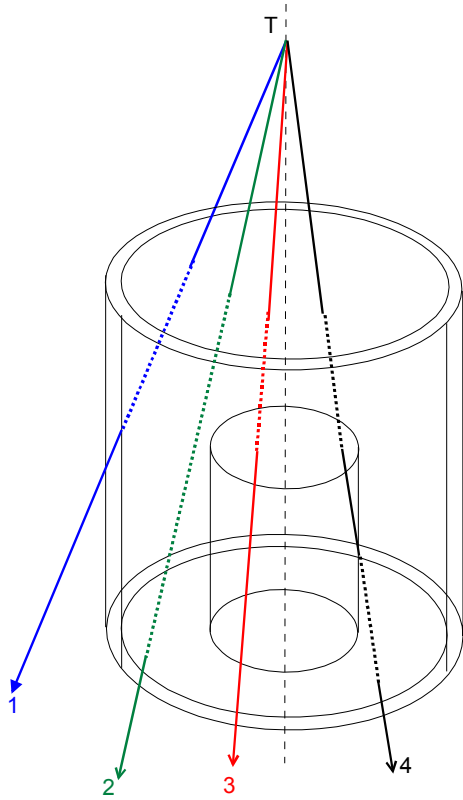


Figure 5 – Sectional diagram of the geometry with a germanium detector and a Marinelli container

Point source

In the case of a point source, the different possible paths of photons emitted by it contributing to the efficiency enter from the front of the detector. Three cases are considered in calculation of the path in the detector:



- no interaction with central hole (Case 1 or 2): the distance travelled is equal to the path from the point of impact to the point of exit;

- interaction with the central hole and exit via the bottom of the hole (Case 3): the distance travelled in the crystal is reduced to the travel up to the central cylinder;

- interaction with the central hole and continuation in the active zone of detection (Case 4): the distance travelled in the detector then consists of two parts; there is also a dead zone component (absorption effect).

Figure 6 – Examples of paths taken into consideration for the point source case

Disk source

The disk source case requires integration over the area of the source. If the radius of the detector is greater than the radius of the source, all paths pass through the front of the detector. Otherwise, it is necessary to add the solid angle sub-tended by the outer ring of the source and the side of the detector.

Paths in the source are similar to those in the point source case with, in addition, the possibility of interaction in the central void occurring at the sides of the cylinder.

Cylindrical source

This case constitutes an extension of the preceding one, with integration of the thickness of the source for calculation of the geometrical solid angle. In addition, for the absorption factors, allowance is being made for the terms due to the material of the source and of the container. Here again, there are two cases, depending on whether the diameter of the source is greater or less than that of the detector.

Marinelli container

The Marinelli container can be divided into two parts: a cylindrical section above the detector window and a hollow cylindrical section surrounding the body of the detector. The first part corresponds to the case covered above, and the second case can, in turn, be divided into three hollow sub-cylinders (Figure 4). The first sub-cylinder is located above the active side of the detector and the radiation from it enters either from the front or from the side of the detector. The second element is characterised by a thickness that is equal to the one of the active zone of detection and the radiation generated in this part mainly enters from the side of the detection crystal. The third sub-cylinder is located below the active zone and radiation paths are detected if they enter from the side or back of the detector.

3. Correction for coincidences

In many experiments, gamma emission probabilities are small and a compromise needs to be made to choose the detector-to-source distance to obtain statistically valid counts. However, it has been observed in experiments that the relative areas of the peaks change with the distance between source and detector, some increasing, others diminishing. This effect is the result of simultaneous detection of X and gamma lines in true coincidence.

The problem is not a new one, and neither are the solutions provided by calculation [1; 8-10]. It is possible to calculate coincidence summing probabilities on the basis of the decay

scheme and the efficiency of the detector at the different energies involved. ETNA represents an update of the CORCO program [1,2] featuring integration of the efficiency calculation part as described in the previous section.

3.1. Effect of coincidences on a photon spectrum

When a radionuclide has a complex decay scheme, the lifetime of the excited levels are generally well below the resolving time of the electronics, and there can be simultaneous detection of pulses resulting from transition cascades. This phenomenon has two different types of effects: loss of counting in the corresponding full-energy peaks and spectra, and creation of additional pulses in the background noise together with energy “sum” peaks equal to the sums of the energies deposited in the detector combined with other counts.

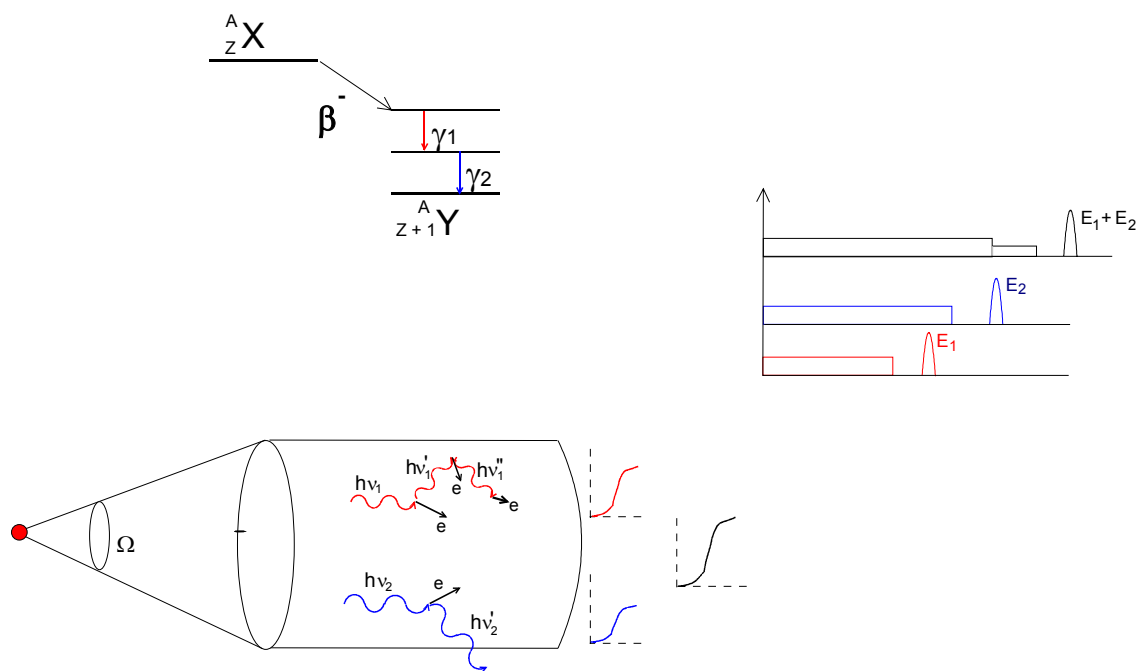


Figure 7 – Effects of coincidence summing in a photon spectrum

Notation: For a transition T_{ij} , the following notation is used:

For the decay scheme:

A: source activity (Bq);

i: upper level (initial) of transition;

j: lower level (final) of transition;

E_{ij} : transition energy;

$P(T_{ij})$: transition probability;

T_i : sum of the probabilities of the transitions incoming to (or leaving) level i ,

α_{ij}^K : K shell internal conversion coefficient for transition i-j;

α_{ij}^T : total internal conversion coefficient;

P_K : K shell capture probability;
 ω_K : K shell fluorescence yield;
 N : maximum level number (levels numbered from 0 to N).

For the detector:

R_{ij}^P : full-energy peak efficiency for energy E_{ij} ;
 R_{ij}^T : total efficiency for energy E_{ij} .

For the spectrum:

N_{ij}^T : number of pulses resulting from total absorption of energy E_{ij} ;
 N'_{ij} : number of pulses actually recorded in the full-energy peak with energy E_{ij} .

3.2. Examples for a decay scheme with two excited levels

Let us consider the basic case of a radionuclide with two excited levels:

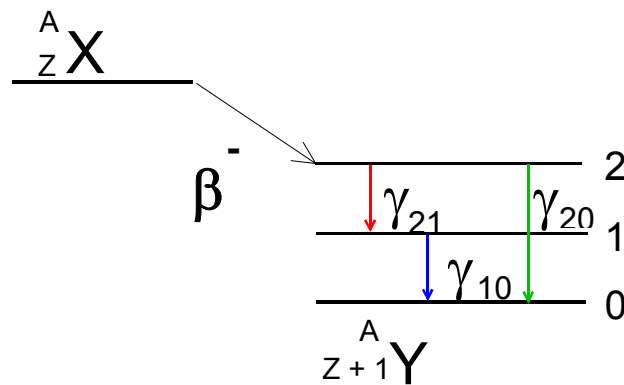


Figure 8 – Decay scheme with two levels

The number of pulses in the detector resulting from total absorption of energy E_{10} corresponding to the transition γ_{10} is the product of the number of photons emitted and the efficiency of the detector for the energy considered, *i.e.*

$$N_{10} = A \cdot \frac{P(T_{10})}{(1 + \alpha_{10}^T)} \cdot R_{10}^P$$

In practice, the possibility of coincidence summing between line γ_{21} and line γ_{10} results in loss of pulses in the peak corresponding to energy E_{10} . The number of lost pulses is proportional to the number of photons emitted which have deposited all their energy in the detector (full-energy peak efficiency), to the probability of coincidence between a 2,1 photon and a 1,0 photon and to the probability of detection of all or part of the energy of the second pulse (total efficiency). This effect results in the actual recording of the number of pulses:

$$N'_{10} = N_{10} - \Delta N_{10} = N_{10} \cdot \left(1 - \frac{P(T_{21})}{T_1 \cdot (1 + \alpha_{21}^T)} \cdot R_{21}^T \right)$$

The correction factor making it possible to re-obtain the true area of the peak corresponding to energy E_{10} can therefore be written as follows:

$$C_{10} = \left(1 - \frac{P(T_{21})}{T_1 \cdot (1 + \alpha_{21}^T)} \cdot R_{21}^T \right)^{-1}$$

The correction factor for the peak corresponding to energy E_{21} is obtained in the same manner,

$$C_{21} = \left(1 - \frac{P(T_{10})}{T_1 \cdot (1 + \alpha_{10}^T)} \cdot R_{10}^T \right)^{-1}$$

However, for the peak corresponding to energy E_{20} , the area recorded is greater than the actual area of the peak:

$$N'_{20} = N_{20} + \Delta N_{20}$$

ΔN_{20} corresponds to a pulse gain associated with the simultaneous absorption of the total energy of the γ_{21} and γ_{10} lines:

$$\Delta N_{20} = A \cdot \frac{P(T_{21})}{(1 + \alpha_{21}^T)} \cdot R_{21}^P \cdot \frac{P(T_{10})}{T_1 \cdot (1 + \alpha_{10}^T)} \cdot R_{10}^P$$

And the correction factor for the total area of the peak corresponding to energy E_{20} is therefore written as follows:

$$C_{20} = \left(1 + \frac{P(T_{21}) \cdot P(T_{10})}{T_1 \cdot P(T_{20})} \cdot \frac{(1 + \alpha_{20}^T)}{(1 + \alpha_{21}^T) \cdot (1 + \alpha_{10}^T)} \cdot \frac{R_{21}^P \cdot R_{10}^P}{R_{20}^P} \right)^{-1}$$

These expressions correspond only to coincidences between gamma emissions. Consideration also needs to be given to the possibilities of coincidence summing with X-ray emissions subsequent to the rearrangements which follow the processes of internal conversion and of electron capture, as well as coincidences between X-ray lines. This extension of the principle rapidly leads to complex expressions for the radionuclides with a decay scheme including numerous cascade transitions. It is therefore necessary to establish general expressions that can be used to reconstitute the decay series and to rapidly calculate the different correction factors.

3.3. General case of a decay scheme with a several excited levels

3.3.1. Correction for a γ_{ij} line

General

For a γ_{ij} line, total correction is calculated with allowance for the possibilities of coincidence with other gamma-ray lines – partial correction $C_{\gamma_{ij}/\gamma}$ and with X-ray lines – partial correction $C_{\gamma_{ij}/X}$ – giving:

$$C_{\gamma_{ij}} = C_{\gamma_{ij}/\gamma} \cdot C_{\gamma_{ij}/X}$$

It is to be noted that the following calculations are first-order approximations as only double coincidences are considered. Indeed, exhaustive calculation would make it necessary to allow for coincidences of order 3 and more. However, as the corresponding corrections are proportional to the product of detection efficiencies which are generally less than 10%, the error resulting from this approximation remains small compared to the uncertainties associated to the other experiment parameters.

Gamma-gamma coincidences

For a γ_{ij} line, the correction factor must allow for all possibilities of coincidence with other gamma emissions. The correction coefficient can be expressed in the form of a three-factor product:

$$C_{\gamma_{ij}/\gamma} = A \cdot B \cdot C$$

A represents the coincidences with gamma-ray lines preceding the γ_{ij} line;

B represents the coincidences with gamma-ray lines following the γ_{ij} line;

C covers coincidences of gamma-ray lines for which the sum of the energies is equal to E_{ij} .

In a decay scheme with $N+1$ levels, designated 0 to N , these factors can be expressed as follows:

$$A = \prod_{l=i}^{N-1} \left[\prod_{k=l+1}^N A_{kl}^{-1} \right] \quad \text{with : } A_{kl} = 1 - \frac{X_{kl}}{T_l} \cdot \frac{R_{kl}^T}{(1 + \alpha_{kl}^T)} \cdot M_{li}$$

$$\text{and } M_{li} = \frac{X_{li}}{T_i} + \sum_{b=i+1}^{l-1} \frac{X_{lb}}{T_b} \cdot M_{bi} \quad (M_{ii} = 1)$$

$$B = \prod_{p=1}^j \left[\prod_{m=0}^{p-1} B_{pm}^{-1} \right] \quad \text{with : } B_{pm} = 1 - \frac{X_{pm}}{T_p} \cdot \frac{R_{pm}^T}{(1 + \alpha_{pm}^T)} \cdot N_{jp}$$

$$\text{and } N_{jp} = \frac{X_{jp}}{T_j} + \sum_{q=p+1}^{j-1} \frac{X_{jq}}{T_j} \cdot N_{qp} \quad (N_{jj} = 1)$$

$$C = \prod_{g=j+1}^{i-1} C_{gj}^{-1} \quad \text{where } C_{gj} = 1 + CF_{gj} + CG_{gj} + CH_{gj}$$

$$\text{with } CF_{gj} = \frac{X_{gj} \cdot X_{ig}}{T_g \cdot X_{ij}} \quad CG_{gj} = \frac{R_{gj}^P \cdot R_{ig}^P}{R_{ij}^P} \quad \text{and} \quad CH_{gj} = \frac{(1 + \alpha_{ij}^T)}{(1 + \alpha_{ig}^T) \cdot (1 + \alpha_{gj}^T)}$$

Gamma and X-ray coincidence summing

The processes of internal conversion and electron capture result in disturbance of the electron cloud of the atom. Rearrangement of it results in emission of X-rays (and Auger electrons) and these can therefore be detected simultaneously with the gamma-ray lines in the same cascade. Thus, for line γ_{ij} , the correction factor for coincidence must allow for,

- coincidences with X-ray lines following internal conversion of transitions preceding γ_{ij} , factor D
- coincidences with X-ray lines following internal conversion of transitions following γ_{ij} , factor E
- coincidences with X-ray lines following the electron capture preceding the γ_{ij} transition, factor F.

The total correction can thus be written as follows:

$$C \gamma_{ij}/X = D \cdot E \cdot F$$

These correction factors are similar to those established for gamma-gamma coincidences, and are obtained by replacing the gamma emission probabilities and the corresponding efficiencies by X-ray emission probabilities and the efficiencies for average X-ray energy.

Note: With the detectors used in gamma spectrometry, the efficiency is practically nil at energy levels corresponding to the XL lines, corrections are therefore only calculated for the XK case.

$$D = \prod_{l=i}^{N-1} \left[\prod_{k=l+1}^N D_{kl}^{-1} \right] \quad \text{with : } D_{kl} = 1 - \frac{X_{kl}}{T_l} \cdot \alpha_{kl}^K \cdot \omega_K \frac{R_{XK}^T}{(1 + \alpha_{kl}^T)} \cdot M_{li}$$

$$E = \prod_{p=1}^j \left[\prod_{m=0}^{p-1} E_{pm}^{-1} \right] \quad \text{with : } E_{pm} = 1 - \frac{X_{pm}}{T_p} \cdot \alpha_{pm}^K \cdot \omega_K \cdot \frac{R_{XK}^T}{(1 + \alpha_{pm}^T)} \cdot N_{jp}$$

$$F = \prod_{l=i}^N F_{Nl}^{-1} \quad \text{with : } F_{Nl} = 1 - \frac{X_{N+1l}}{T_l} \cdot (P_K)_{N+1l} \cdot \omega_K \cdot R_{XK}^T \cdot M_{li}$$

In these expressions, M_{li} and N_{jp} are expressed in the same manner as in the gamma-gamma coincidence case.

3.3.2. Correction for XK lines

The X-ray lines correspond to the processes of electron capture and internal conversion. Although of different origins, the corresponding corrections are calculated in the same manner if the index $n+1$ is assigned to the initial level of electron capture. The total correction for all the X-ray lines, C_X , therefore represents the contribution of the elementary corrections C_{Xij} associated with internal conversion of a γ_{ij} transition and the $C_{X_{n+1}j}$ elementary corrections corresponding to capture of an electron leading to excited nuclear level j .

$$C_X = \frac{\sum_{i=1}^N \sum_{j=0}^{i-1} C_{Xij} \cdot X_{ij} \cdot \frac{\alpha_{ij}^K}{(1 + \alpha_{ij}^T)}}{\sum_{i=1}^N \sum_{j=0}^{i-1} X_{ij} \cdot \frac{\alpha_{ij}^K}{(1 + \alpha_{ij}^T)}} + \frac{\sum_{j=1}^N C_{X_{n+1}j} \cdot X_{N+1,j} \cdot P_{KN+1,j}}{\sum_{j=1}^n X_{N+1,j} \cdot P_{KN+1,j}}$$

X-gamma coincidences

Although they result from electron capture or internal conversion, X-ray lines can coincide with gamma-ray lines in the same way as different gamma-ray lines can coincide. The corrections are therefore calculated in a manner similar to that described above:

$$C_{Xij}/\gamma = A \cdot B \quad \text{for internal conversion}$$

$$C_{X_{n+1}j}/\gamma = B \quad \text{for electron capture}$$

X-X coincidences

Calculation of corrections for X-ray lines coincidences is performed in the same manner as for coincidences between gamma and X-ray lines, *i.e.*

$C_{X_{ij}/X} = D \cdot E \cdot F$ for internal conversion

$C_{X_{n+1,j}/X} = E$ for electron capture

3.4. Special cases

3.4.1. Beta+ emission

After a beta+ emission, recombination of the positron with an electron results in the emission of two annihilation photons of 511 keV, which can coincide with X- and gamma-ray lines in the same cascade. This case is dealt with by using a modified scheme [9], including an additional virtual level and an i-j transition with the following characteristics:

$$E_{ij} = 511 \text{ keV}$$

$$\alpha_{ij}^T = -0.5 \text{ (in order to allow for the simultaneous emission of two photons)}$$

$$\text{and } P(X_{ij}) / T_i = 1$$

3.4.2. Decay scheme with two branches

For a radionuclide characterised by a decay scheme with two branches (for instance, ^{152}Eu decays by beta minus emission into excited levels of ^{152}Gd and by electron capture to those of ^{152}Sm), no difficulties are encountered: all that is required is to consider the two branches separately. However, it must be verified that the energy of a sum peak observed for one of the two branches does not correspond to the energy of a transition in the other branch.

Thus, for instance, for ^{152}Eu , the simultaneous detection of gamma-ray lines of 122 and 245 keV (^{152}Sm branch) gives rise to a sum peak overlying a peak corresponding to a gamma-ray line with an energy of 368 keV (^{152}Gd branch). In both cases, it is necessary to apply the correction factor only to the part of the peak involved (^{152}Sm branch).

3.4.3. Decay scheme with one metastable level

The existence of a metastable level with a lifetime greater than the electronic resolving time of the measuring system prevents the phenomenon of coincidence summing for transitions located on either side of the level. For it to be taken into account, it is necessary to add an additional level on which higher transitions arrive, with a nil probability of transition between the virtual level and the metastable level (from which the lower transitions originate) to prevent any coincidence between transitions on either side of the level.

3.5. Case of non-point samples

The coincidence correction calculation described below assumes that the sample is a point, that it is located at a distance from the detector used for reference and for which the detector is calibrated in terms of efficiency. However, for other conditions of measurement than those of calibration, the variation in efficiency can be determined from variations in the geometrical

parameters of the source-detector system. This reasoning can be applied to determine the efficiency for elemental volume sources at different points, then calculate the coincidence summing corrections by integrating the contributions for the entire volume. Thus, for an element of volume dV , located at position r , it is easy to transpose the basic relationships established for a point source with a decay scheme with two excited levels :

$$N_{10}(r)dV = A(r) \cdot \frac{P(T_{10})}{(1 + \alpha_{10}^T)} \cdot R_{10}^P(r) dV$$

$$N'_{10}(r) dV = N_{10}(r) \cdot \left(1 - \frac{P(T_{21})}{T_1 \cdot (1 + \alpha_{21}^T)} \cdot R_{21}^T(r) \right) dV$$

If the activity is uniformly distributed in the source, integration over volume V of the source gives

$$N_{10} = \frac{A}{V} \cdot \frac{P(T_{10})}{(1 + \alpha_{10}^T)} \cdot \int_V R_{10}^P(r) dV$$

and

$$N'_{10} = \frac{A}{V} \cdot \frac{P(T_{10})}{(1 + \alpha_{10}^T)} \cdot \left(\int_V R_{10}^P(r) dV - \frac{P(T_{21})}{T_1(1 + \alpha_{21}^T)} \int_V R_{10}^P(r) R_{21}^T(r) dV \right)$$

From which it is possible to deduce the correction factor:

$$C_{10} = \left(1 - \frac{P(T_{21})}{T_1(1 + \alpha_{21}^T)} \cdot \frac{\int_V R_{10}^P(r) R_{21}^T(r) dV}{\int_V R_{10}^P(r) dV} \right)^{-1}$$

Correction factors C_{21} and C_{10} can be written in the same way:

$$C_{21} = \left(1 - \frac{P(T_{10})}{T_1(1 + \alpha_{10}^T)} \cdot \frac{\int_V R_{21}^P(r) R_{10}^T(r) dV}{\int_V R_{21}^P(r) dV} \right)^{-1}$$

$$C_{20} = \left(1 + \frac{P(T_{21})P(T_{10})}{T_1 P(T_{20})} \cdot \frac{(1 + \alpha_{20}^T)}{(1 + \alpha_{21}^T)(1 + \alpha_{10}^T)} \cdot \frac{\int_V R_{21}^P(r) R_{10}^P(r) dV}{\int_V R_{20}^P(r) dV} \right)^{-1}$$

The same reasoning applies to the case of a radionuclide characterised by a complex decay scheme with n levels and can be used to obtain general relationships in the same manner as in

the point source case. Thus, for a line ij coinciding with a line kl, the total efficiency R_{kl}^T has to be replaced by the relationship:

$$I = \frac{\int_V R_{ij}^P(r) R_{kl}^T(r) dV}{\int_V R_{ij}^P(r) dV}$$

This algorithm thus includes the elemental efficiencies which are calculated using the method described for efficiency transfer (see §2).

4. Description of the program

4.1. General

The ETNA program runs under Windows®. It consists of two parts: the interface and the calculation engine. The interface, made with Visual Basic, enables the user to enter the necessary parameters for calculation in a user-friendly manner by means of a succession of descriptive windows. It includes databases containing linear attenuation coefficients of materials derived from the XCOM program [7] and decay data derived from the “Nucléide” table [11] containing all the decay scheme data necessary for calculation of coincidence summing corrections. It also creates, when required, a user database concerning the transfer and calibration configuration parameters. The use of the program is described in the user manual, covering the user interface in detail [see Appendix 2]. The calculation engine, written in Fortran, carries out the processing described above. It consists of three dynamic link libraries called by the Visual Basic module: ETNA_ET for efficiency transfer, ETNA_CSC_SP for full calculation of coincidence corrections, and ETNA_CSC_SL for simplified calculation of coincidence corrections. In this last case, the program first makes an efficiency transfer calculation for the conditions of measurements and then calculates the corrections as for a point source.

The two modules are linked by means of ASCII files generated for input by the Visual Basic part containing the parameters necessary for the Fortran engines. In turn, the results of calculation are returned from the Fortran engine to the Visual Basic interface for display and recording of the results.

The file FICGEO.DAT is used for the three calculation engines. This contains the geometrical data. The first line contains codes for identifying the type of geometry transfer, then the detector characteristics. The second and third lines contain the calibration and measurement geometry characteristics respectively.

Code (ITYP)	Calibration geometry	Transfer geometry
1	Point source	Point source

2	Point source	Disk source
3	Point source	Cylindrical source
4	Point source	Marinelli source
5	Disk source	Point source
6	Disk source	Disk source
7	Disk source	Cylindrical source
8	Disk source	Marinelli source
9	Cylindrical source	Point source
10	Cylindrical source	Disk source
11	Cylindrical source	Cylindrical source
12	Cylindrical source	Marinelli source
13	Marinelli source	Point source
14	Marinelli source	Disk source
15	Marinelli source	Cylindrical source
16	Marinelli source	Marinelli source

First line : Detector data:

DIADE	Crystal diameter (cm)	Real (2 numbers + 2 decimals)
EPAIDE	Crystal thickness (cm)	Real (2 numbers + 2 decimals)
EPAIZM	Dead layer thickness (cm)	Real (1 numbers + 4 decimals)
DISCF	Crystal-window distance (cm)	Real (1 numbers + 4 decimals)
EPAIFE	Window thickness (cm)	Real (1 numbers + 4 decimals)
DAVI	Hole diameter (cm)	Real (2 numbers + 2 decimals)
EPAIVI	Hole thickness (cm)	Real (2 numbers + 2 decimals)
DIACAP	End-cap diameter (cm)	Real (2 numbers + 2 decimals)
EPAICAP	End-cap thickness (cm)	Real (2 numbers + 2 decimals)

Second line: calibration geometry characteristics:

DISREF	Calibration distance (cm)	Real (5 numbers + 4 decimals)
DIASOR	Container diameter (cm)	Real (3 numbers + 2 decimals)
EPAISOR	Container thickness (cm)	Real (3 numbers + 2 decimals)
DIAMINR	Container hole diameter (Marinelli) (cm)	Real (2 numbers + 2 decimals)
PROFINR	Container hole thickness (Marinelli) (cm)	Real (2 numbers + 2 decimals)
EPAIFOR	Container bottom thickness (cm)	Real (2 numbers + 2 decimals)
EPAICOR	Container internal wall thickness (Marinelli) (cm)	Real (2 numbers + 2 decimals)
DISECR	End-cap –to shield distance (cm)	Real (2 numbers + 2 decimals)
EPAIECR	Shield thickness (cm)	Real (1 numbers + 4 decimals)

Third line: measurement geometry characteristics:

DISMES	Transfer distance (cm)	Real (5 numbers + 4 decimals)
DIASOM	Container diameter (cm)	Real (3 numbers + 2 decimals)
EPAISOM	Container thickness (cm)	Real (3 numbers + 2 decimals)
DIAMINM	Container hole diameter (Marinelli) (cm)	Real (2 numbers + 2 decimals)
PROFINM	Container hole thickness (Marinelli) (cm)	Real (2 numbers + 2 decimals)
EPAIFOM	Container bottom thickness (cm)	Real (2 numbers + 2 decimals)
EPAICOM	Container internal wall thickness (Marinelli) (cm)	Real (2 numbers + 2 decimals)
DISECM	End-cap –to shield distance (cm)	Real (2 numbers + 2 decimals)
EPAIECM	Shield thickness (cm)	Real (1 numbers + 4 decimals)

The file FICANG.DAT is used for efficiency transfer. This consists of one line per energy level considered, including the following information:

K	Energy number	Integer (2 numbers)
---	---------------	---------------------

ENE	Transition energy	Real (5 numbers + 6 decimals)
RDT	Detector efficiency for the transition energy in calibration conditions.	Real (5 numbers + 6 decimals)
CAGE	Linear attenuation coefficient of the crystal for the transition energy	Real (5 numbers + 6 decimals)
CAFE	Linear attenuation coefficient of the window for the transition energy	Real (5 numbers + 6 decimals)
CACE	Linear attenuation coefficient of the end-cap for the transition energy	Real (5 numbers + 6 decimals)
CAAIR	Linear attenuation coefficient of the calibration environment for the transition energy	Real (5 numbers + 6 decimals)
CASOR	Linear attenuation coefficient of the calibration source for the transition energy	Real (5 numbers + 6 decimals)
CACOR	Linear attenuation coefficient of the calibration container for the transition energy	Real (5 numbers + 6 decimals)
CAECR	Linear attenuation coefficient of the calibration shield for the transition energy	Real (5 numbers + 6 decimals)
CAAIM	Linear attenuation coefficient of the measurement environment for the transition energy	Real (5 numbers + 6 decimals)
CASOM	Linear attenuation coefficient of the measurement source for the transition energy	Real (5 numbers + 6 decimals)
CACOM	Linear attenuation coefficient of the measurement container for the transition energy	Real (5 numbers + 6 decimals)
CAECM	Linear attenuation coefficient of the measurement shield for the transition energy	Real (5 numbers + 6 decimals)

The file FICCOR.DAT is used by the coincidence correction engines. It contains the decay series data with two lines containing general data followed by one line per gamma transition:

First line containing general data:

NOMNIV	Number of the maximal level	Integer (2 numbers)
OMEGAK	K Fluorescence yield	Real (1 number + 4 decimals)
OMEGAL	L Fluorescence yield	Real (1 number + 4 decimals)
ENERGX	XK mean energy	Real (3 number + 2 decimals)
ENERGL	XL mean energy	Real (3 number + 2 decimals)
EFATOX	Full-energy peak efficiency for XK energy	Real (1 number + 6 decimals)
EFTOX	Total efficiency for XK energy	Real (1 number + 6 decimals)
EFATOL	Full-energy peak efficiency for XL energy	Real (1 number + 6 decimals)
EFTOL	Total efficiency for XL energy	Real (1 number + 6 decimals)

Second line containing general data:

COATGEX	Linear attenuation coefficient of the crystal for XK energy	Real (5 numbers + 6 decimals)
COATFEX	Linear attenuation coefficient of the window for the XK energy	Real (5 numbers + 6 decimals)
COATCAX	Linear attenuation coefficient of the end-cap for the XK energy	Real (5 numbers + 6 decimals)
COATAIXR	Linear attenuation coefficient of the calibration environment for the XK energy	Real (5 numbers + 6 decimals)
COATSOXR	Linear attenuation coefficient of the calibration source for the XK energy	Real (5 numbers + 6 decimals)
COATCOXR	Linear attenuation coefficient of the calibration container for the XK energy	Real (5 numbers + 6 decimals)
COATECXR	Linear attenuation coefficient of the calibration shield for the XK energy	Real (5 numbers + 6 decimals)
COATAIXM	Linear attenuation coefficient of the measurement environment for the XK energy	Real (5 numbers + 6 decimals)
COATSOXM	Linear attenuation coefficient of the measurement source for the XK energy	Real (5 numbers + 6 decimals)
COATCOXM	Linear attenuation coefficient of the measurement container for the XK energy	Real (5 numbers + 6 decimals)
COATECXM	Linear attenuation coefficient of the measurement shield for the XK energy	Real (5 numbers + 6 decimals)

	energy	
COATGEL	Linear attenuation coefficient of the crystal for XL energy	Real (5 numbers + 6 decimals)
COATFEL	Linear attenuation coefficient of the window for the XL energy	Real (5 numbers + 6 decimals)
COATCAL	Linear attenuation coefficient of the end-cap for the XL energy	Real (5 numbers + 6 decimals)
COATAILR	Linear attenuation coefficient of the calibration environment for the XL energy	Real (5 numbers + 6 decimals)
COATSOLR	Linear attenuation coefficient of the calibration source for the XL energy	Real (5 numbers + 6 decimals)
COATCOLR	Linear attenuation coefficient of the calibration container for the XL energy	Real (5 numbers + 6 decimals)
COATECLR	Linear attenuation coefficient of the calibration shield for the XL energy	Real (5 numbers + 6 decimals)
COATAILM	Linear attenuation coefficient of the measurement environment for the XL energy	Real (5 numbers + 6 decimals)
COATSOLM	Linear attenuation coefficient of the measurement source for the XL energy	Real (5 numbers + 6 decimals)
COATCOLM	Linear attenuation coefficient of the measurement container for the XL energy	Real (5 numbers + 6 decimals)
COATECLM	Linear attenuation coefficient of the measurement shield for the XL energy	Real (5 numbers + 6 decimals)

Data concerning a gamma-ray line (in one line):

K	Number of the starting level	Integer (2 numbers)
L	Number of the arriving level	Integer (2 numbers)
ENE	Transition energy	Real (5 numbers + 6 decimals)
TRAN	Transition intensity	Real (5 numbers + 6 decimals)
SOM	Sum of the transition intensities of the transitions starting for the upper level	Real (5 numbers + 6 decimals)
COINK	Internal conversion coefficient in K shell	Real (5 numbers + 6 decimals)
COINL	Internal conversion coefficient in L shell	Real (5 numbers + 6 decimals)
COTO	Total conversion coefficient	Real (5 numbers + 6 decimals)
EAT	Full-energy peak efficiency	Real (5 numbers + 6 decimals)
EFT	Total efficiency	Real (5 numbers + 6 decimals)
CAG	Linear attenuation coefficient of the crystal for the transition energy	Real (5 numbers + 6 decimals)
CAF	Linear attenuation coefficient of the window for the transition energy	Real (5 numbers + 6 decimals)
CAC	Linear attenuation coefficient of the end-cap for the transition energy	Real (5 numbers + 6 decimals)
CAIR	Linear attenuation coefficient of the calibration environment for the transition energy	Real (5 numbers + 6 decimals)
CASR	Linear attenuation coefficient of the calibration source for the transition energy	Real (5 numbers + 6 decimals)
CACR	Linear attenuation coefficient of the calibration container for the transition energy	Real (5 numbers + 6 decimals)
CAER	Linear attenuation coefficient of the calibration shield for the transition energy	Real (5 numbers + 6 decimals)
CAIM	Linear attenuation coefficient of the measurement environment for the transition energy	Real (5 numbers + 6 decimals)
CASM	Linear attenuation coefficient of the measurement source for the transition energy	Real (5 numbers + 6 decimals)
CACM	Linear attenuation coefficient of the measurement container for the transition energy	Real (5 numbers + 6 decimals)
CAEM	Linear attenuation coefficient of the measurement shield for the transition energy	Real (5 numbers + 6 decimals)

All three calculation modules output a file named FICSOR.DAT. For efficiency transfer, this includes one line per energy with the initial efficiency (calibration), the transfer coefficient and the efficiency calculated for the measurement geometry. In the case of corrections of

coincidences, it includes a first line with a global correction for X-ray emissions, then a line for each transition of the decay scheme including energy, gamma-gamma correction, gamma-X correction and total correction (the product of the two separate contributions).

4.2. Calculation of efficiency transfer

Knowing the different geometrical parameters of the source-detector system for the conditions of calibration and measurement, the program calculates the correction factor to be applied to the efficiency, *i.e.* the ratio of the effective solid angles (see §2.1). It is therefore possible to change from one geometry to another with the same detector and point, disk, cylinder or Marinelli sources resulting in 12 possible combinations. For each energy, the software successively calculates the two solid angles and returns the ratio of the two and the new efficiency (product of calibration efficiency and correction factor). Provision is made for different detector materials (GeHP, Si(Li), NaI(Tl) etc.) provided that they are of cylindrical coaxial geometry.

The calculation time varies with the geometry. Depending on the power of the computer, it can range from a few seconds for the simplest cases (point to point) involving, for each geometry, two integration loops and calculation of five distances, to a number of minutes for more complex cases (Marinelli to Marinelli) necessitating five integrations and calculation of seven distances for each iteration.

4.3. Calculation of coincidence-summing corrections

Calculation of coincidence summing corrections is performed for a given radionuclide and a given source-detector geometry. It is necessary to know the calibration for total and full-energy peak efficiency for a reference geometry and for the energy range concerned. The decay scheme is reconstituted from basic data including the total number of levels, the fluorescence efficiency values, the X-ray emission energies and the different transitions, as well as, for each, the final and initial levels, the probability of photon emission and the conversion coefficients in the different atomic shells. The efficiencies corresponding to the energies of the different transitions are interpolated on the basis of known discrete values. In the case of non-point sources, the calculations include integration for elementary efficiencies, the determination of which necessitates knowledge of the attenuation coefficients of the different materials on the paths of the photons. Once again, the required coefficients, for the energies involved in the decay series, are interpolated from tabulated discrete values.

As in the case of efficiency calculation, overall processing time varies greatly, depending on the geometry involved and, especially, the complexity of the decay scheme, as the program processes all the lines of the scheme in the same procedure.

5. Conclusion

The ETNA program is designed to meet the requirements of users for whom gamma spectrometry analysis accuracy is important. Featuring a user-friendly interface, it can

calculate the detection efficiency of a source-detector system with coaxial cylindrical geometry on the basis of efficiency calibration for reference conditions. In addition, it can be used to calculate the coincidence-summing corrections to be applied to experimental counting rates that are substantially disturbed for radionuclides with complex decay scheme and for short-range geometry (the case of measurement of environmental samples with low levels of activity).

The quality of the results provided by ETNA depends mainly on the quality of the reference calibration and, when geometry transfer is necessary, on the precise knowledge of the geometrical parameters of the source-detector system.

The accuracy of the efficiency calculations was tested in the Euromet initiative [12,13] for transfer from a point source geometry at a reference distance to other distances and to cylindrical geometries with different matrixes. The results show that, for the test cases, the differences between the values calculated and the experimental values are not more than 2 to 3% in the worst cases (low energies), which is amply sufficient for most routine measurement work.

6. Bibliography

- [1] J. MOREL, B. CHAUVENET and A. KADACHI
Coincidence summing corrections in gamma-ray spectrometry for normalized geometries
Int. J. Appl. Radiat. Isot. 34/8 (1983) 1115-1122.
- [2] M.C. LÉPY, J. MOREL and B. CHAUVENET
Corrections des pertes de comptage dues aux coïncidences gamma-gamma, gamma-X et X-X dans un spectre de photons. Rapport CEA-R-5356 (1986)
- [3] L. MOENS, J. DE DONDER, LIN Xi-lei, F. DE CORTE, A. DE WISPELAERE, A.SIMONITS and J. HOSTE
Calculation of the absolute peak efficiency of gamma-ray detectors for different counting geometries. Nucl. Instrum. Meth. 187 (1981) 451-472.
- [4] S. JOVANOVIĆ, A. DLABAC, N. MIHALJEVIĆ and P. VUKOTIĆ
ANGLE : A PC-code for semiconductor detector efficiency calculations. J. of Radioanal. and Nucl. Chem, Vol 218, N°1, (1997) 13-20.
- [5] L. ABRAMOWITZ and I.A. STEGUN
Handbook of mathematical functions with formulas, graphs and mathematical tables.
Ed. Wiley (1972)
- [6] O. SIMA
Application of Monte Carlo calculations to gamma-spectrometric measurements of environmental samples. Appl. Radiat. Isot 47 N°9/10 (1997) 919
- [7] M.J. BERGER and J.H. HUBBELL
XCOM : Photon cross sections on personal computers. NBSIR 87-3597
- [8] D.S. ANDREEV, K.I. EROKHINA, V.S. ZVONOV and I. KH. LEMBERG
Consideration of cascade transitions in determining the absolute yield of gamma rays.
Izv. Akad. Nauk. SSSR Ser. Fiz. 37 N°8 (1973) 1609
- [9] G.H. MCCALLUM and G.E. COOTE
Influence of source-detector distance on relative intensity and angular correlation measurements with Ge(Li) spectrometers. Nucl. Instrum. Meth. 130 (1975) 189-197.
- [10] K. DEBERTIN and U. SCHÖTZIG
Coincidence summing corrections in Ge(Li) spectrometry at low source-to-detector distances
Nucl. Instrum. Meth 158 (1979) 471-477.
- [11] M.M. BÉ, E. BROWNE, V. CHECHEV, N. COURSOL, B. DUCHEMIN, R. HELMER, J. LAMÉ, C. MORILLON, F. PITON and E. SCHÖNFELD
Table de Radionucléides, Volume 5, CEA/DAMRI, 91191 Gif-sur-Yvette, France. 1999, ISBN 2 7272 0200 8

NUCLEIDE, Table de Radionucléides sur CD-Rom, Version 1-98, CEA/DAMRI, 91191 Gif-sur-Yvette, France.

[12] F. PITON, M.C. LEPY, M.M. BE and J. PLAGNARD
Efficiency transfer and coincidence summing corrections for gamma-ray spectrometry
Appl. Radiat. Isot., 52 (2000) 791-795.

[13] Rapport EUROMET
M.C. LEPY AND ALL THE PARTICIPANTS OF THE EUROMET ACTION 428
Transfer of Ge detectors efficiency calibration from point source geometry to other geometries EUROMET ACTION 428. Rapport CEA-R-5894 (2000)

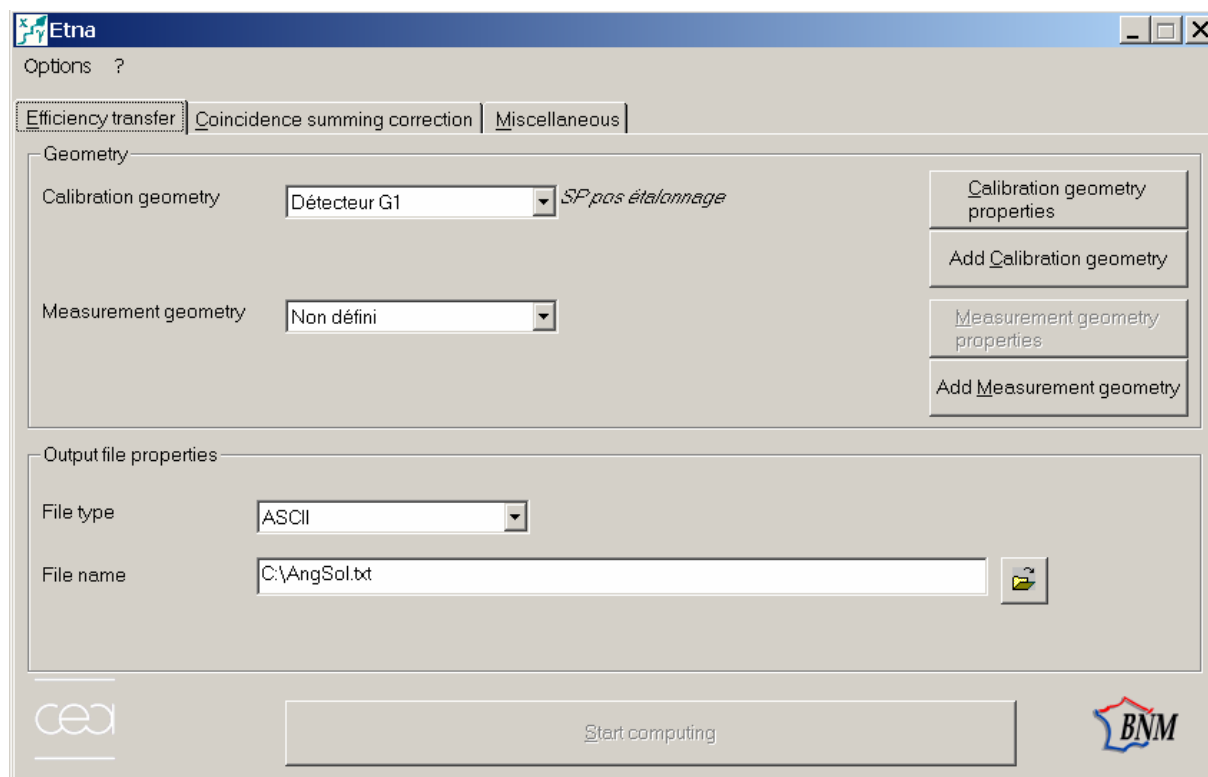
APPENDIX 1 – User manual

A1_1 General

The ETNA program simplifies gamma spectrometry by calculating efficiency transfers when the source-detector geometry is changed and when it is necessary to make corrections for coincidence summing for radionuclides with complex decay scheme.

The program is installed by launching the program “setup.exe” in the sub-directory “SETUP”. A dialogue then appears for setting the installation directory (by default : “C:\Program Files\ETNA”), and creates two sub-directories (“MOTOR” and “DATABASE”); the first one includes the computation programs (ETNA_ET.DLL, ETNA_CSC_SP.DLL and ETNA_CSC_SL.DLL) and the last one contains databases necessary for carrying out the different processings (ETNA_SYS.MDB, ETNA_USR.MDB, ETNA_MAC.MDB et ETNA_NUC.MDB).

The program is launched in Windows by clicking on “etna.exe” in the created directory “ETNA” or on its icon. The following dialogue then appears:



The top toolbar contains two buttons marked “Options” and “?”. The first one allows to define users's preferences : the language in which the program messages are displayed (French or English) is selected by clicking the button marked “Language”. The paths used for the databases and the output files are selected by clicking the "Paths" button.



The button marked “?” (About) causes information to appear concerning the versions of the calculation modules and the program interface.

The input window has three main tabs corresponding to the two calculation modules and one utility module:

- Efficiency transfer
- Coincidence summing corrections
- Miscellaneous

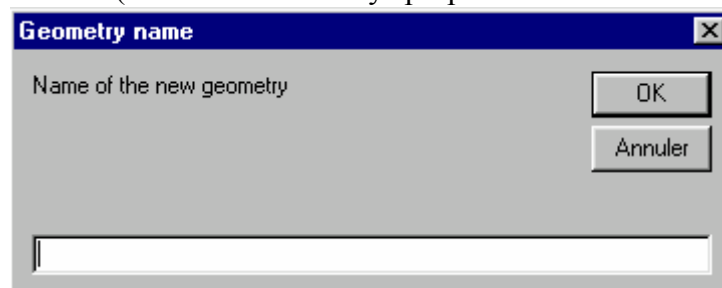
By default, the efficiency transfer tab is selected.

A1_2 Efficiency transfer

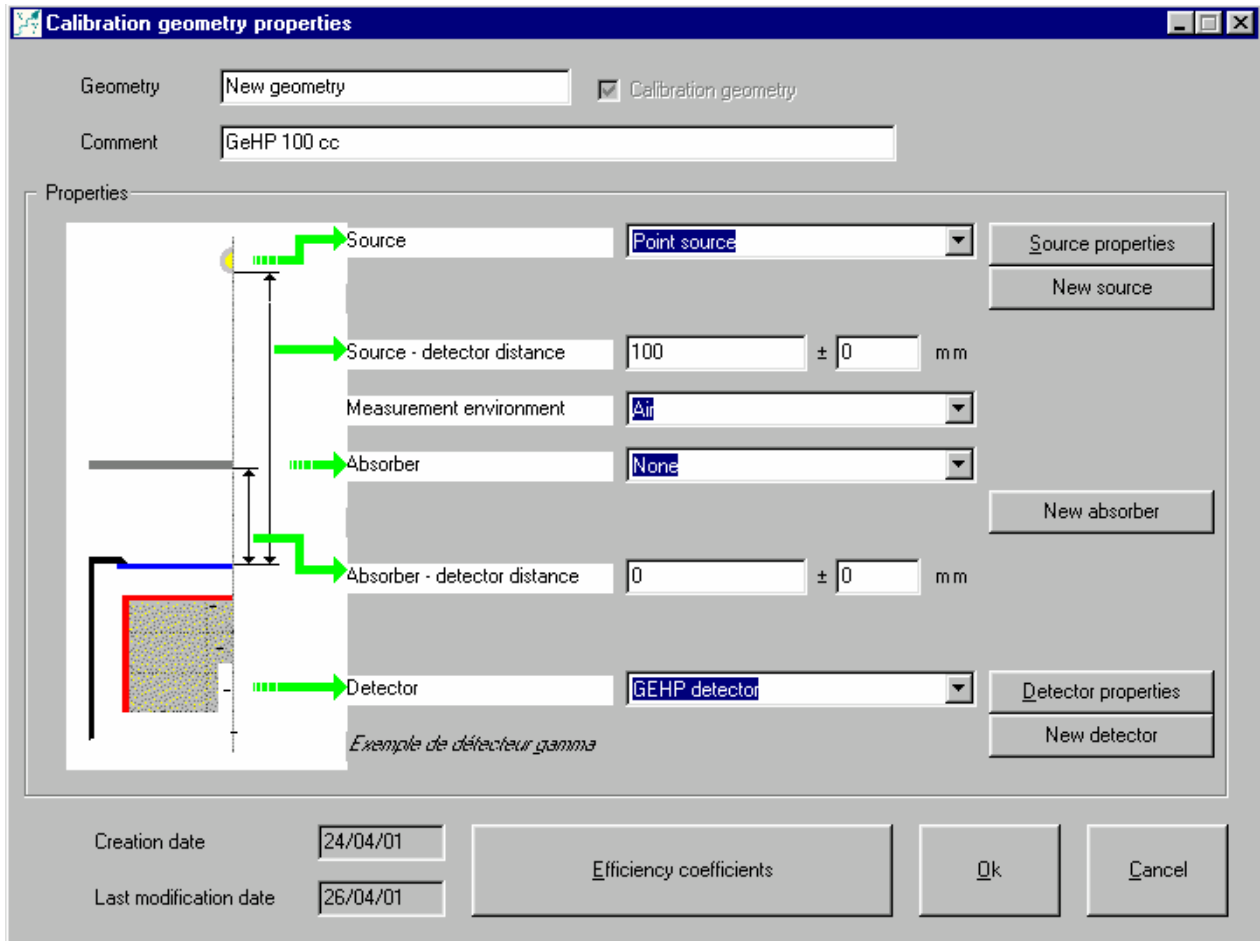
The efficiency calculation module is used to calculate the coefficient of transfer of efficiencies from one geometry to another, with a cylindrical detector and a coaxial geometry source-detector system. This calculation necessitates knowledge of the geometrical parameters of the source-detector system, for reference conditions (calibration geometry) and for transfer conditions (measurement geometry).

For each of the geometries (calibration and measurement), a popup list is available for selecting a previously-recorded geometry and displaying its properties. This appears when the button marked “Properties of the geometry” is clicked. When the button marked “New geometry” is clicked, new geometry parameters can be entered after entering an identifier (one identifier per geometry):

Two buttons are provided (marked “Geometry properties” and “New geometry”) for



accessing a window entitled “Geometry properties”. With the first button, the various parameters can be read and modified; with the second button, they are entered by the user.

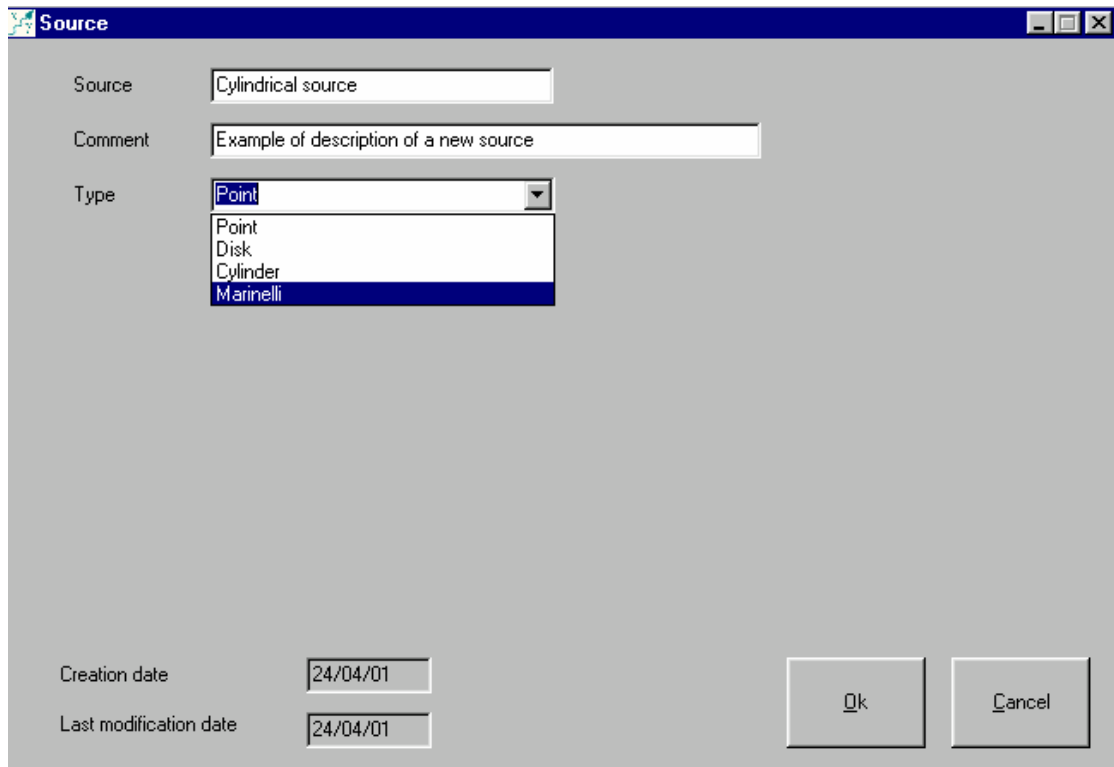


It is therefore required to:

- describe the source,
- state the source-detector distance,
- state the measurement environment (in air by default),
- state whether an absorber is present or not: if it is, it needs to be described and its distance from the detector window must be indicated,
- describe the detector.

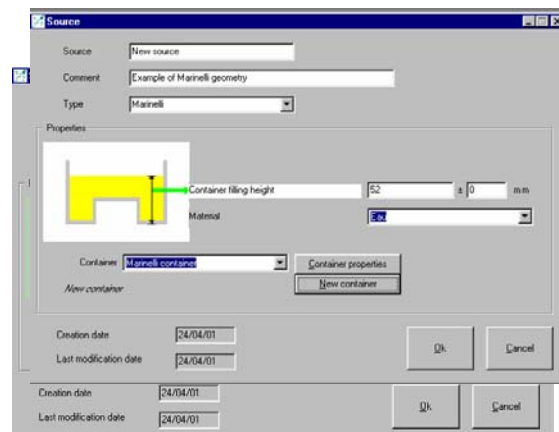
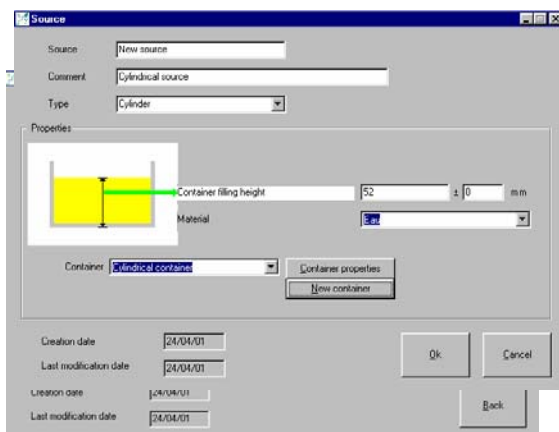
The various parameters are entered either by picking from a popup list (for pre-existing objects), entered directly in a field, or entered by creating a new object after clicking the button marked “New source”, “New absorber” or “New detector”.

A1_2.1 Description of the source

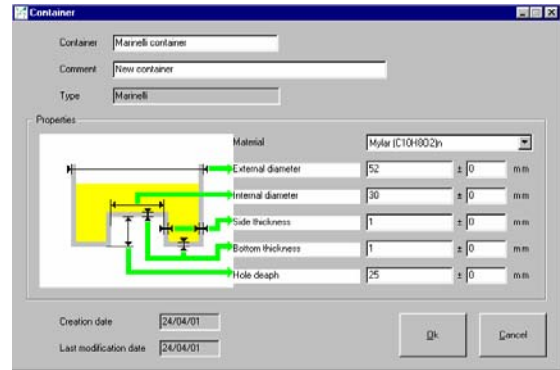
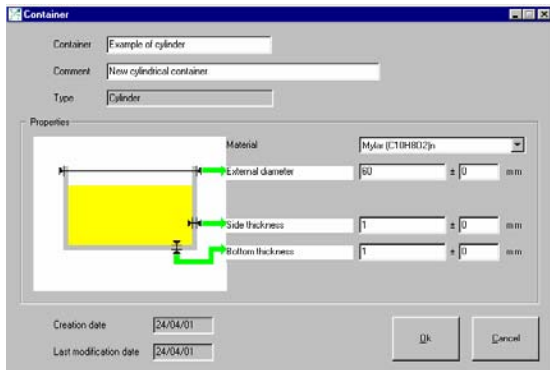


The following window is used to select the source geometry (point, disk, cylinder or Marinelli); then, if it is not a point source, a new window appears for entering the following parameters:

Disk source	Cylinder source	Marinelli source
Diameter	<i>Source material</i>	<i>Source material</i>
	Height of filling	Height of filling
	<i>Container material</i>	<i>Container material</i>
	Container diameter	Outside diameter of container
	Thickness of side wall	Inside diameter of container
	Thickness of bottom wall	Thickness of side wall
		Thickness of bottom wall
		Depth of hole



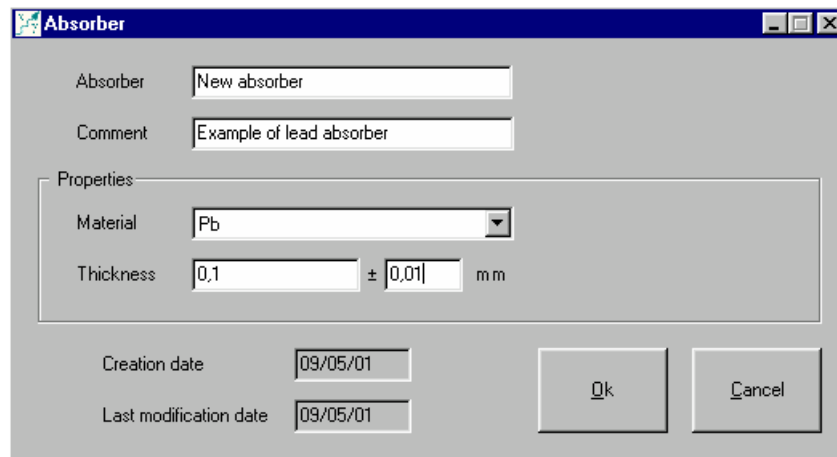
In the case of a volume source, it is also necessary to describe the container (cylinder or Marinelli):



A1_2.2 Description of the absorber

In the same way, it is possible to display the properties of an absorber or create a new one and its characteristics:

Absorber
<i>Absorber material</i>
Absorber thickness



A1_2.3 Description of the detector

The detector constitutes the last (and most important) part of the geometry. As before, its properties are introduced either by means of popup lists (for materials) or by directly entering the geometrical dimensions in the appropriate fields:

Detector
<i>Crystal material</i>
Crystal diameter
Crystal thickness

Dead zone thickness
Hole diameter
Hole depth
<i>Window material</i>
Window thickness
Window-crystal distance
<i>Cover material</i>
Cover thickness
Cover diameter

Detector properties

Detector:

Detector comment:

Detector side cap thickness:

Window material:

Window thickness: ± mm

Crystal - window distance: ± mm

Crystal dead zone top thickness: ± μm

Crystal material:

Crystal thickness: ± mm

Crystal hole depth: ± mm

Crystal hole diameter: ± mm

Crystal diameter: ± mm

Detector side cap thickness: ± mm

Detector side cap diameter: ± mm

Detector side cap material:

Creation date:

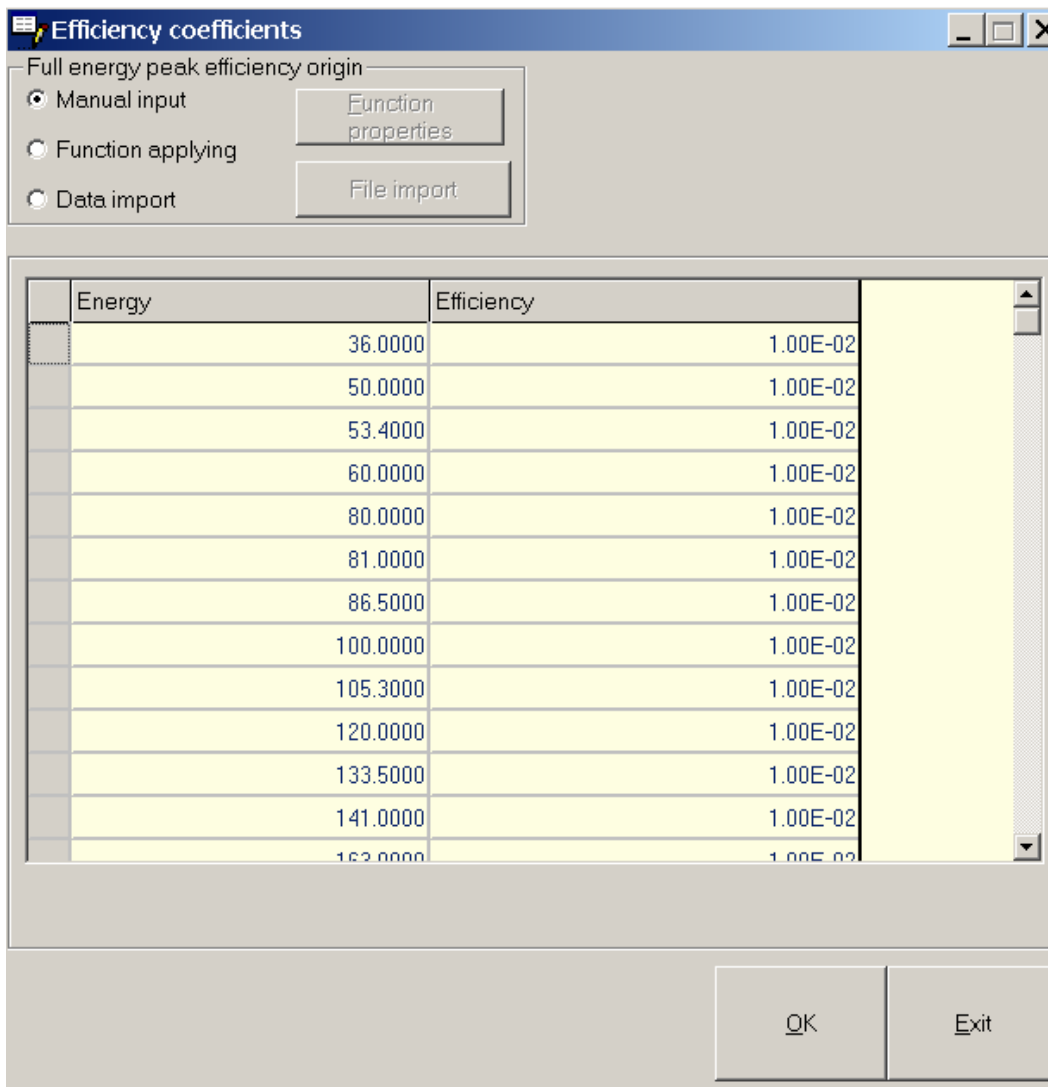
Last modification date:

These parameters are generally given on the detector datasheet supplied by the manufacturer.

A certain number of commonly-used materials are included in the database (see §4) which contains the linear attenuation coefficients and density, and are available in the material pick list for the source and its container, the absorber, and the detector crystal, window and cover. New materials can be added to these lists in the “materials management” module.

A1_2.4 Efficiency

If a calibration geometry is described, it is important to state the corresponding efficiency values for reference purposes. To do so, a new window is opened by clicking on the button marked “Efficiency coefficients” in the screen “geometry properties”. The values are entered either step by step in a predefined energy table, either using an expression representing variation of the efficiency as a function of energy, or importing data from an external file :

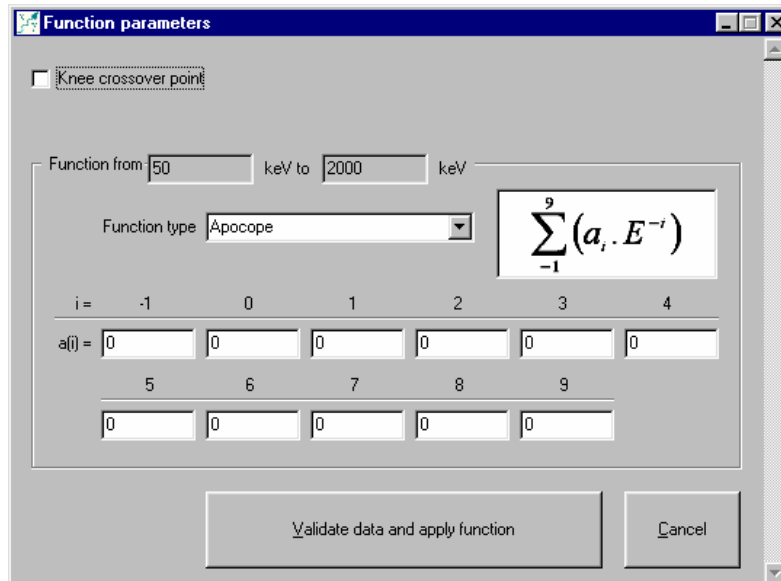


To apply an efficiency function , two formulas commonly used in gamma spectrometry are proposed:

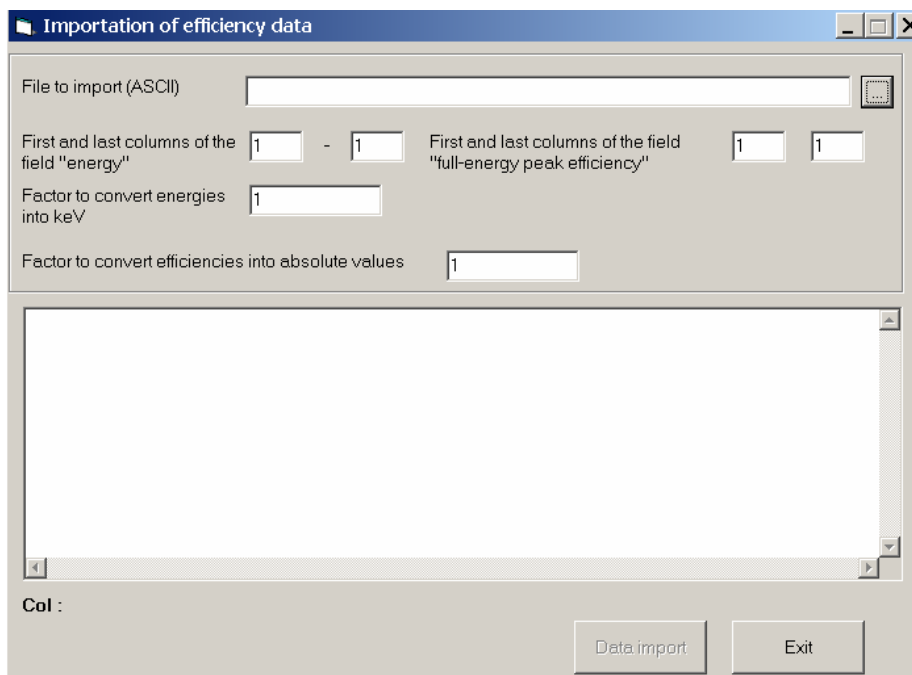
$$\text{APOCOPE: } \ln R^P(E) = \sum_{i=0}^n a_i \cdot E^{-i}$$

$$\text{APOLOG: } \ln R^P(E) = \sum_{i=0}^n a_i \cdot (\ln E)^i$$

The function is then selected and its coefficients a_i are entered for the energies, in keV. In this case, it is possible to adopt a cut-off point beyond which the coefficients are different.



Importation of external data requires an external file (ASCII) including data for energy and efficiency stored in columns :

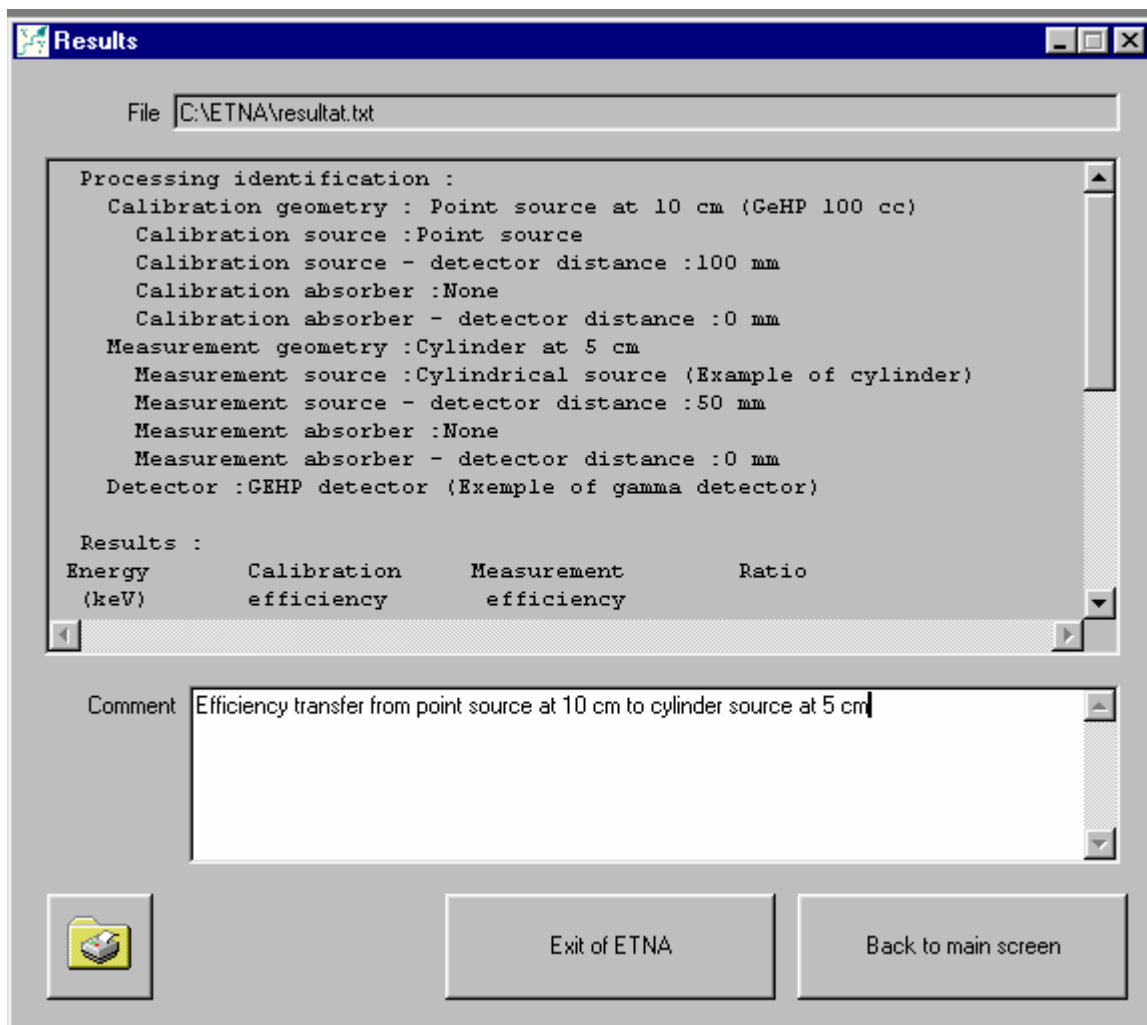


After deleting the unneeded lines of data (by highlighting them then pressing the “delete” key on the keyboard), the required columns of the external file are selected by indicating their positions (beginning and end), as well as the conversion factors necessary for the energies to be expressed in keV and the efficiency in absolute value.

By default, the efficiency is initialised at 10^{-2} , and the program can calculate the coefficient for transfer from one geometry to another with these values. If the true efficiency values for the calibration geometry are entered, the program calculates the transfer coefficient and the actual efficiency values for the measurement geometry.

A1_2.5 Processing

The calculation module is launched by clicking on the button marked “Start computing” after selecting a calibration geometry and a transfer geometry. The results are displayed on the screen and can be printed out. They are also recorded in a file which can subsequently be read. The file is of the ASCII or Excel type and its path is indicated in the window.



The processing time depends on the geometries involved, particularly the complexity of the source, as calculation includes integrations for all its dimensions.

The results file contains the calculation conditions for reference, the efficiencies for the calibration conditions and the results, *i.e.* the coefficients of transfer and the new efficiencies for the energy set-up selected:

ETNA _____ v5.0 - 09/02/2001

Filename :C:\ETNA\resultat.txt

Processing identification :

Calibration geometry : Point source at 10 cm (GeHP 100 cc)
Calibration source :Point source
Calibration source - detector distance :100 mm
Calibration absorber :None
Calibration absorber - detector distance :0 mm
Measurement geometry :Cylinder at 5 cm
Measurement source :Cylindrical source (Example of cylinder)
Measurement source - detector distance :50 mm
Measurement absorber :None
Measurement absorber - detector distance :0 mm
Detector :GEHP detector (Exemple of gamma detector)

Results :

Energy (keV)	Calibration efficiency	Measurement efficiency	Ratio
00050,000	00,01000000	00,00875331	00,87533100
00080,000	00,01000000	00,01045363	01,04536300
00100,000	00,01000000	00,01083164	01,08316400
00120,000	00,01000000	00,01109121	01,10912100
00150,000	00,01000000	00,01125043	01,12504300
00200,000	00,01000000	00,01150021	01,15002100
00300,000	00,01000000	00,01189691	01,18969100
00400,000	00,01000000	00,01219106	01,21910600
00500,000	00,01000000	00,01242986	01,24298600
00600,000	00,01000000	00,01261905	01,26190500
00800,000	00,01000000	00,01291247	01,29124700
01000,000	00,01000000	00,01313099	01,31309900
01200,000	00,01000000	00,01330345	01,33034500
01500,000	00,01000000	00,01350731	01,35073100
02000,000	00,01000000	00,01375149	01,37514900

Comment :

Efficiency transfer from point source at 10 cm to cylinder source at 5 cm
CEA\LNHB _____ BNM

A1_3 Corrections for coincidence summing

The coincidence corrections calculation module calculates the correction factors to be applied to recorded peak areas for a given radionuclide and source-detector geometry. It is activated by selecting the tab marked “Coincidence summing corrections”, which causes the following window to open:

The screenshot shows the 'Etna' software window with the 'Coincidence summing correction' tab selected. The interface includes the following elements:

- Options:** Efficiency transfer, Coincidence summing correction (selected), Miscellaneous.
- Nuclide:** Ag110 (selected in dropdown).
- Daughter nuclide:** Cd110 (selected in dropdown).
- Geometry:**
 - Calibration geometry:** Non défini (selected in dropdown). Buttons: Calibration geometry properties, Add Calibration geometry.
 - Measurement geometry:** (empty dropdown). Buttons: Measurement geometry properties, Add Measurement geometry.
 - Measurement geometry different from calibration geometry.
- Output file properties:**
 - File type:** ASCII (selected in dropdown).
 - File name:** C:\Corco.txt (text input field). Button: Save.
- Bottom Panel:**
 - Logos: ceo, BNM.
 - Radio buttons: Simplified computing (selected), Complete computing.
 - Button: Start computing.

The calculation necessitates knowing the decay scheme of the radionuclide and the two efficiencies, full-energy peak and total, for the source-detector arrangement.

A1_3.1 Radionuclide

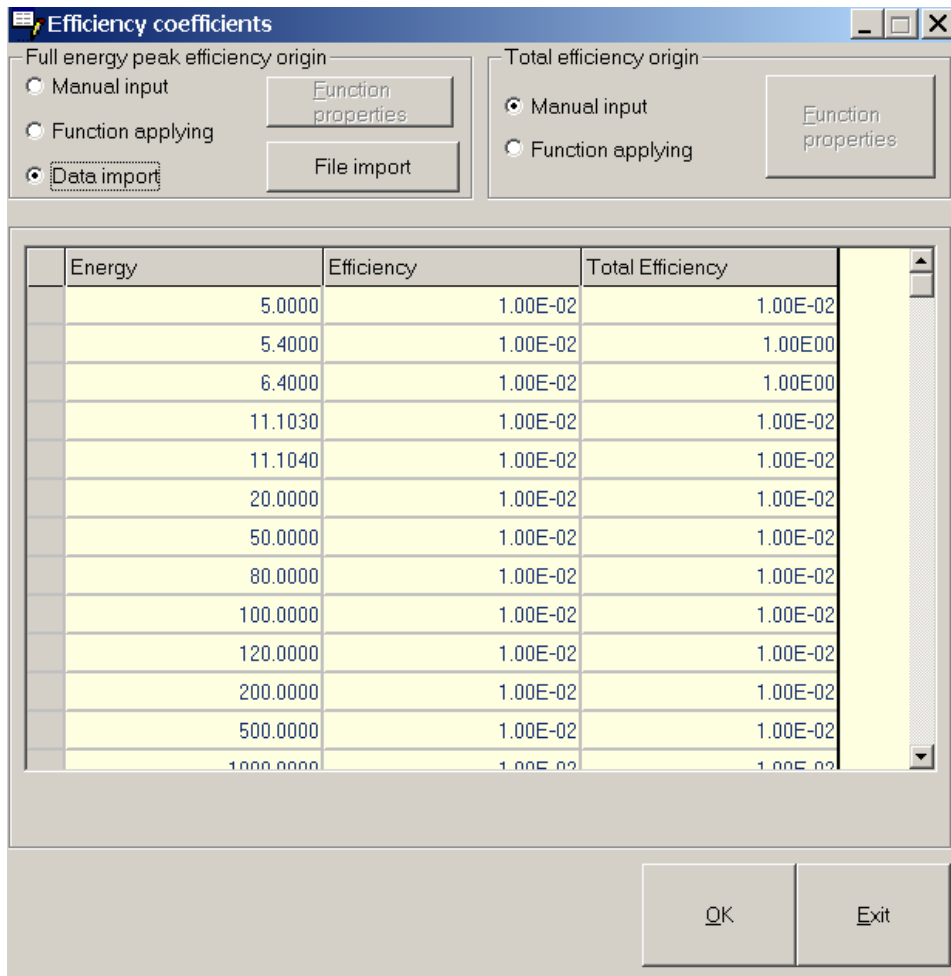
The radionuclide is selected from a popup list. If there are two decay branches, it is also necessary to select the daughter nuclide.

A1_3.2 Geometry

Two cases can arise:

Either the efficiencies are known for the working geometry,

Or they are known for a reference geometry, in which case the program must make the efficiency transfer corresponding to the geometry change. It is therefore necessary to indicate the geometrical parameters of the source-detector system, for the reference conditions and for the calculation conditions. The parameters are entered in the same manner as for efficiency transfer (see §2), except that, in this case, it is necessary to enter the values (or the formulas) of the two efficiencies (total and full-energy peak) for the program to run.

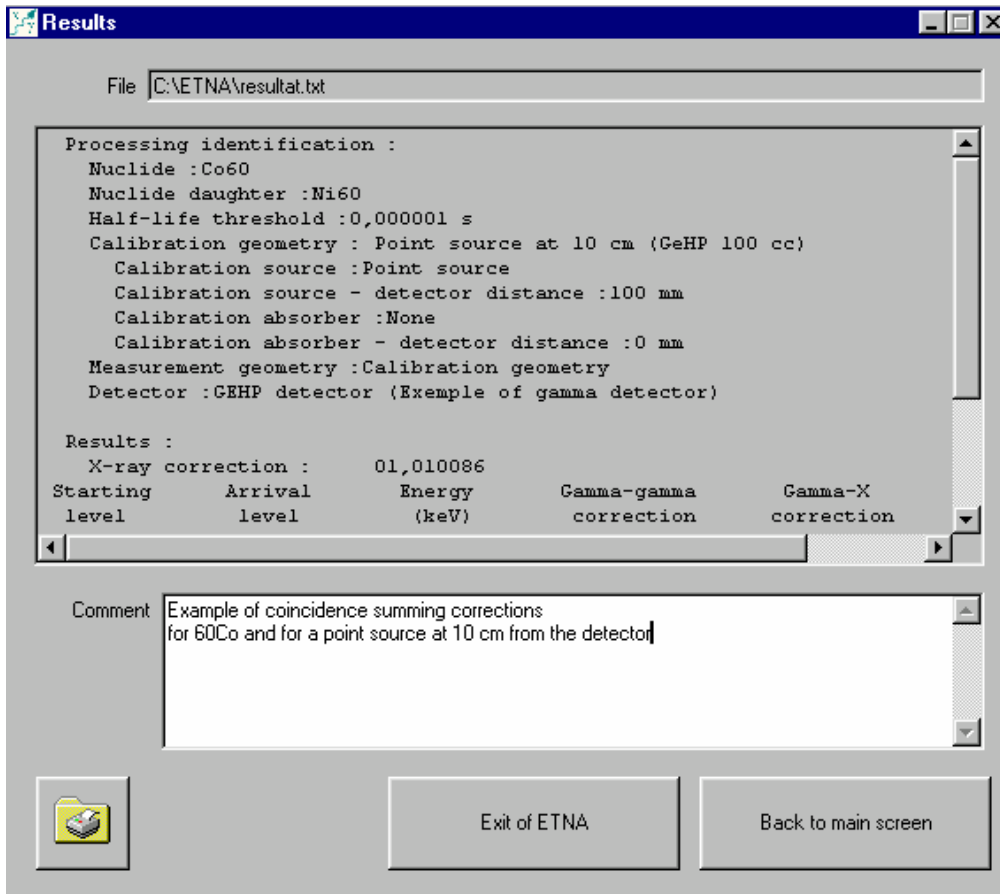


By default, the efficiency values are initialised at 10^{-2} , but unlike in the efficiency transfer case, the true values of the efficiencies must be entered to obtain significant results.

A1_3.3 Processing

The calculation module is launched by clicking the button marked “Start computing” after selecting a radionuclide, a calibration geometry and a measurement geometry if it is different from the calibration geometry. Two options are available: full calculation or rapid calculation. In the second case, the processing includes approximations to accelerate the calculation. Caution is required as this may be detrimental to the precision of the results with high-volume geometries.

The results are displayed on the screen and can be printed out. They are also recorded in a file which can subsequently be read. The file is of the ASCII or Excel type and its path is indicated in the window.



Overall resulting ASCII file :

ETNA _____ v5.0 - 09/02/2001

Filename :C:\ETNA\resultat.txt

Processing identification :

Nuclide :Co60
 Nuclide daughter :Ni60
 Half-life threshold :0,000001 s
 Calibration geometry : Point source at 10 cm (GeHP 100 cc)
 Calibration source :Point source
 Calibration source - detector distance :100 mm
 Calibration absorber :None
 Calibration absorber - detector distance :0 mm
 Measurement geometry :Calibration geometry
 Detector :GEHP detector (Exemple of gamma detector)

Results :

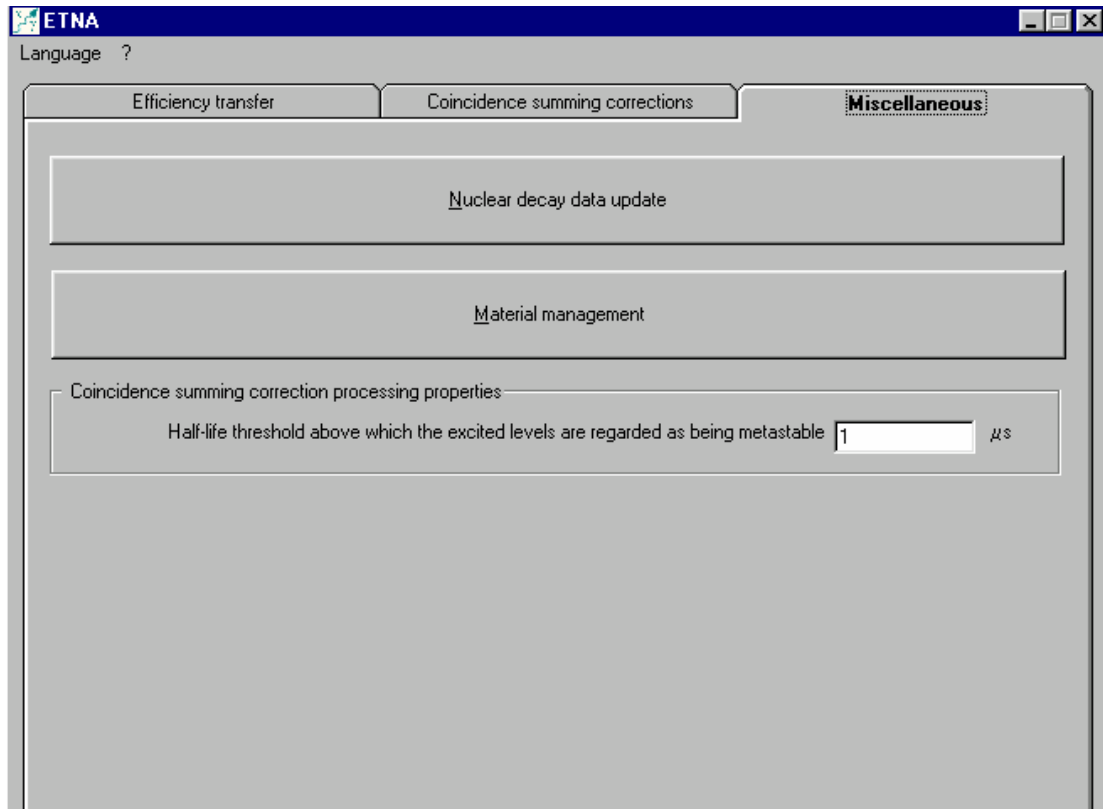
Starting level	Arrival level	Energy (keV)	Gamma-gamma correction	Gamma-X correction	Total correction
001	000	01332,508	01,010086	01,000001	01,010086
002	000	02158,610	00,948501	01,000018	00,948518
002	001	00826,100	01,018734	01,000018	01,018753
003	000	02505,748	00,000000	01,000000	00,000000
003	001	01173,240	01,010099	01,000000	01,010100
003	002	00347,140	01,018884	01,000002	01,018886

Comment :

Example of coincidence summing corrections
 for 60Co and for a point source at 10 cm from the detector
 CEA\LNHB _____ BNM

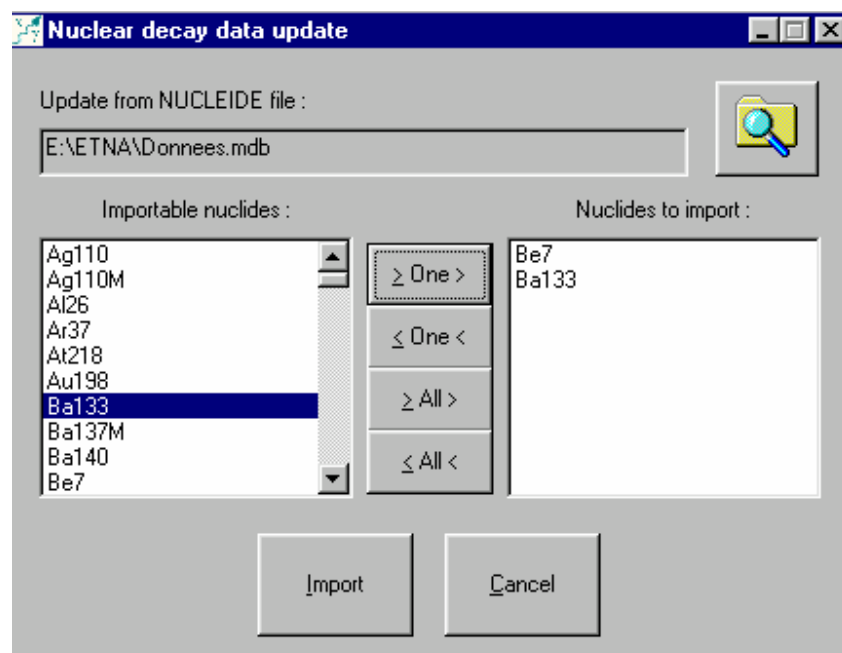
A1_4 Miscellaneous

The miscellaneous tab gives access to two modules which can be used to update the data used for calculation (decay scheme data and linear attenuation coefficients) and for setting a threshold for coincidence summing correction calculation:



A1_4.1 Updating of decay data

Decay data are constantly evolving and the radionuclide table [11] is regularly updated. It is accordingly possible to read the data (file “donnees.mdb”) and import it into the ETNA database:



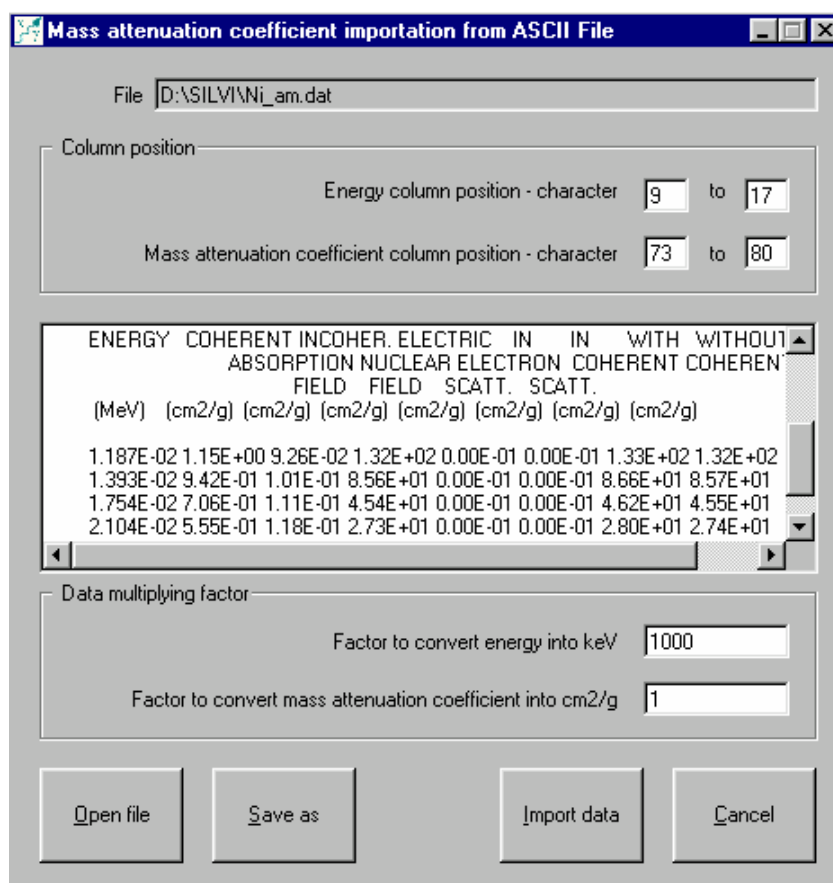
A1_4.2 Materials management

The materials management window gives access to the list of materials used by the program; for each, the following information is available: mass per unit volume, list of linear attenuation coefficients for a pre-established set of energies, and the different components of the source-detector geometry in which the material can occur.

The screenshot shows a window titled "Material management" with a standard Windows-style title bar. At the top, there is a navigation bar with left and right arrow buttons and a text field containing "Material database - record :1/117". To the right of this is a "New" button. Below the navigation bar is a section for "Material properties" containing a "Material identifier" field with "Actinium (Ac)", a "Specific mass" field with "10,05" and "g/cm3", and a "Suppress" button. Underneath is a "Material of" section with several checkboxes: "Detector crystal", "Source", "Absorber", "Detector window", "Container", "Measurement environment", and "Side cap". The main part of the window is a table with two columns: "Energy (keV)" and "Mass attenuation coefficient (cm2/g)". The table contains 12 rows of data. Below the table is a checkbox labeled "Mass attenuation coefficients reading from ASCII file", with "Update" and "Cancel" buttons to its right. At the bottom of the window, there are two date fields: "Creation date" and "Last modification date", both showing "07/09/99", and a "Back" button on the right.

Energy (keV)	Mass attenuation coefficient (cm ² /g)
1,000E+00	6,460E+03
1,039E+00	6,020E+03
1,080E+00	5,610E+03
1,081E+00	5,690E+03
1,171E+00	4,880E+03
1,269E+00	4,190E+03
1,270E+00	4,280E+03
1,500E+00	3,070E+03
2,000E+00	1,680E+03
3,000E+00	6,870E+02
3,219E+00	5,850E+02
3,220E+00	1,530E+03

These lists can be read, edited and added to. For the linear attenuation coefficients, it is possible to import the data contained in the external file, in ASCII format, consisting of two columns containing energy and coefficient data:



After deleting the unneeded lines of data (by highlighting them then pressing the “delete” key on the keyboard), the required columns of the external file are selected by indicating their positions (beginning and end), as well as the conversion factors necessary for the energies to be expressed in keV and the linear attenuation coefficients in $\text{cm}^2 \cdot \text{g}^{-1}$. In the basic version of ETNA, the coefficients are taken from the XCOM program.

A1_4.3 Setting the threshold for calculation of coincidence corrections

Coincidence phenomena occur when the lifetimes of nuclear levels are substantially less than the electronic resolving time of the acquisition system. By default, levels with a lifetime greater than 1 microsecond are considered to be metastable, *i.e.* that they do not give rise to coincidence phenomena. If the characteristics of the acquisition system make it necessary, the value of the threshold can be modified by means of the field provided.

APPENDIX 2 – Definitions

A2_1 Data characterising the decay scheme

A2_1.1 Gamma transition

A gamma transition corresponds to the process of de-excitation of a nucleus at a given energy state (E_i) to a less energetic state or to the ground state (E_j). This transition is accompanied by the emission of either a gamma photon (γ) or a conversion electron (EC), or more rarely, if possible in terms of energy, by the emission of an electron-positron pair (e^\pm).

The probability of transition, $P(T_{ij})$, is the probability of de-excitation of the nucleus occurring by this transition, hence:

$$P(T_{ij}) = P(\gamma_{ij}) + P(EC_{ij}) + P(e^\pm_{ij})$$

$P(\gamma_{ij})$, $P(EC_{ij})$ and $P(e^\pm_{ij})$ are intensities of emission of a gamma photon, a conversion electron or an electron-positron pair respectively.

A2_1.2 Gamma emission

In this process, the energy of the gamma transition is converted into electromagnetic radiation in the form of an energy photon E_{ij} :

$$E_{ij} = (E_i - E_j) - E_r$$

$(E_i - E_j)$ represents the energy difference between the initial and final states, i.e. between the gamma transition and E_R , the recoil energy of the final nucleus:

$$E_R = \frac{(E_i - E_j)^2}{2Mc^2}$$

M being the mass of the nucleus.

The intensity of gamma emission $P(\gamma_{ij})$ corresponds to the ratio between the number of gamma photons emitted per transition T_{ij} and the number of spontaneous nuclear transitions (or disintegrations).

A2_1.3 Internal conversion

The transition energy is communicated to an electron of an atom, which is then ejected with a kinetic energy of:

$$E_c = E_{ij} - W$$

Where W represents the binding energy of the electron in the relevant shell.

The intensity of internal conversion electron emission, $P(EC_{ij})$, corresponds to the number of conversion electrons emitted per transition T_{ij} divided by the number of spontaneous nuclear transitions.

The total internal conversion coefficient, α_{ij}^T , corresponds to the ratio between the intensity of conversion electron emission and the intensity of gamma emission:

$$\alpha_{ij}^T = \frac{P(EC_{ij})}{P(\gamma_{ij})}$$

The K-shell internal conversion coefficient, α_{ij}^K , corresponds to the ratio between the intensity of K shell conversion electron emission, $P(EC_{Kij})$, and the intensity of gamma emission:

$$\alpha_{ij}^K = \frac{P(EC_{Kij})}{P(\gamma_{ij})}$$

The partial internal conversion coefficients α_{ij}^L , α_{ij}^M , etc. corresponding to shells L, M, etc. are defined in a similar way, hence the relationship:

$$\alpha_{ij}^T = \alpha_{ij}^K + \alpha_{ij}^L + \alpha_{ij}^M$$

A2_1.4 X-Ray emission following internal conversion

The process of internal conversion gives rise to vacancies in the electron cloud. A vacancy is filled by transfer of an electron from a less strongly bonded shell to the shell where the gap has appeared. During this rearrangement, the transfer of additional energy results in the emission of an X-photon or ejection of an Auger electron.

The K shell fluorescent yield, ω_K , corresponds to the probability of filling of a vacancy in K shell being accompanied by emission of an X_K photon:

$$\omega_K = \frac{P(X_K)}{N_K}$$

Where $P(X_K)$ represents the number of X_K photons emitted and N_K , the number of vacancies in K shell.

For a transition T_{ij} , the intensity of emission of a X_K photon, $P(X_{Kij})$, can therefore be written as follows:

$$P(X_{Kij}) = \frac{\alpha_{ij}^K}{1 + \alpha_{ij}^T} \cdot \omega_K \cdot T(\gamma_{ij}) = \alpha_{ij}^K \cdot P(\gamma_{ij}) \cdot \omega_K$$

A2_1.5 Electron capture

This disintegration process is characterised by the capture of an orbital electron by the nucleus:



Capture of an electron is far more probable in K shell than in the outer shells.

The probability of electron capture, P(CE), is defined as the probability of disintegration of the active nucleus occurring by electron capture. This is also associated with the probabilities of capture P_K , P_L , P_M , etc. for the different electron shells K, L, M, etc. such as that:

$$P_K + P_L + P_M + \dots = 1$$

Like internal conversion, electron capture results in disturbance of the electron cloud, and its rearrangement results in the emission of X photons or Auger electrons. Therefore, the intensity of emission of an X_K photon after electron capture can be written as follows:

$$P(X_K) = P_K \cdot \omega_K$$

A2_2 Parameters characterising the detector

The quantitative analysis of a photon spectrum depends on the knowledge of the detector response in terms of efficiency for the considered geometry.

A2_2.1 Full-energy peak efficiency

R_{ij}^P corresponds to the ratio between the number of events recorded in the total absorption peak corresponding to energy E_{ij} , and the number of γ_{ij} photons emitted by the source.

A2_2.2 Total efficiency

R_{ij}^P is the ratio between the number of events recorded in the entire spectrum and the number of γ_{ij} photons emitted by the source.